Christoph Mittag

Role of intralaminar thalamic neurons during spike and wave discharges in a genetic rat model of absence epilepsy

2010

Biologie

Dissertationsthema

Role of intralaminar thalamic neurons during spike and wave discharges in a genetic rat model of absence epilepsy

Inaugural-Dissertation
zur Erlangung des Doktorgrades
der Naturwissenschaften im Fachbereich Biologie
der Mathematisch-Naturwissenschaftlichen Fakultät
der Westfälischen Wilhelms-Universität Münster

vorgelegt von
Christoph Mittag
aus Wiesbaden
-2010-

Dekanin/Dekan:	Prof. Dr. C. Klämbt
Erste Gutachterin/ Erster Gutachter:	Prof. Dr. H.-C. Pape
Zweite Gutachterin/ Zweiter Gutachter:	Prof. Dr. N. Sachser
Tag der mündlichen Prüfung(en):	27.09.2010.....…….....
Tag der Promotion:	22.10.2010……..

Table of contents

1. Introduction

Rhythms are one central element of life. A well known example is the rhythm given by sleep and wakefulness. For both states, the thalamus is of overall importance. It is a structure in the diencephalon and consists of several nuclei. Each nucleus gets input from specific afferent signal (e.g. visual or auditory sensory information) and transmits them to specific areas of the cortex. In such a way, nearly all information we are aware of have to pass the thalamus (an exception being olfactory information). Thus, the thalamus is in an ideal position to act as a gateway, where incoming signals are either transferred to the cortex, or blocked. During wakefulness the thalamus transfers incoming sensory signals, whereas during sleep, the flow of information from the periphery to the cortex is interrupted within the thalamus (Jones, 1985; Sherman and Guillery, 2006). Because of its ability to control the flow of information in dependence of sleep and wakefulness, the thalamus is often viewed as "the gate to consciousness" (Pape et al., 2005).

1.1 Physiological properties of the thalamus

Early electrophysiological studies, using sharp intracellular microelectrodes, showed that thalamic neurons fire in two different modes, depending on their membrane potential (Jahnsen and Llinas, 1984a, b, c). During membrane potentials negative to -60 mV, representing the hyperpolarized state, neurons generated a single burst of spikes, whereas tonic repetitive firing was produced from membrane potentials positive to -60 mV, representing the depolarized state (Fig. 1.1).

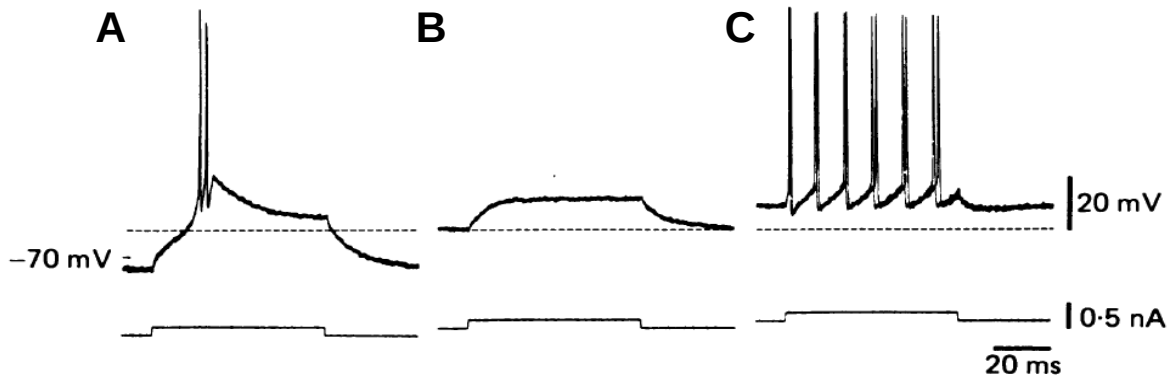

Fig. 1.1: Firing properties of a thalamic neuron. **A)** During hyperpolarization, the current pulse triggers an all-or-none burst of spikes. **B)** The same current pulse causes a subthreshold depolarization when the membrane potential was slightly depolarized. **C)** After further depolarization, the current pulse evokes a train of action potentials. Upper traces show the membrane potential of the recorded neuron, lower traces represent the injected current. Figure from Jahnsen and Llinas (1984b).

When thalamic neurons are depolarized they operate in the transfer mode, in which the frequency of action potentials follows natural stimulation in a linearly proportional way. This activity reflects the state of wakefulness: incoming signals to the thalamus are directly relayed to the cortex. During the hyperpolarized state, neurons operate in the oscillatory mode, which dominates the resting states of drowsiness and quiet sleep. In that mode, the membrane potential is characterized by long lasting hyperpolarizations interrupted by burst discharges. Depolarizing stimuli result in stereotypical burst discharges (Steriade and Deschenes, 1984; Steriade and Llinas, 1988). The oscillatory mode and the transfer mode can be distinguished by its characteristic waveform in the electroencephalogram (EEG). In the oscillatory mode, burst discharges are accompanied by an EEG of low frequency and high amplitude. Characteristic of the transfer mode is an EEG of high frequency and low amplitude. (Fig. 1.2).

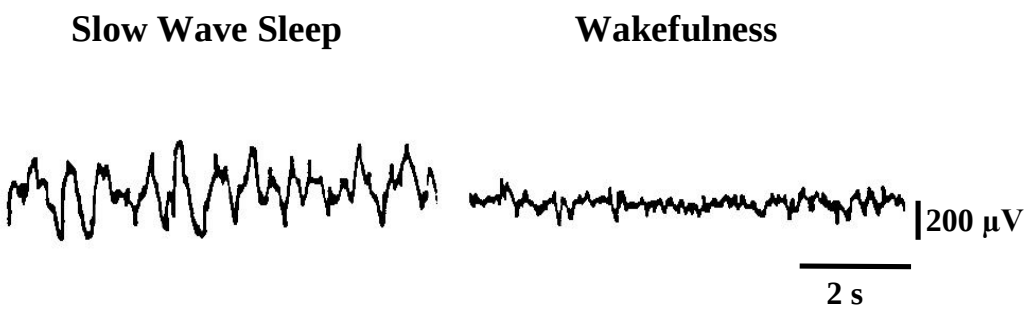

Fig. 1.2: EEG recordings from cats, during sleep and wakefulness. Adapted from McCormick and Bal (1997).

Different types of oscillatory waveforms have been described, including sleep spindles, delta waves, and slow oscillations. Slow oscillations (<1 Hz) are generated in the cortex and are a result of prolonged hyperpolarization of cortical neurons followed by a depolarized phase. In that way, they provide the envelope in which the other waveforms are nested (Hobson and Pace-Schott, 2002; Steriade and Timofeev, 2003). Delta waves (1-4 Hz), which are prominent during deep sleep stages, can either be generated through intrinsic mechanisms by thalamocortical projection neurons or they can be produced within the cortex (McCormick and Bal, 1997; Hobson and Pace-Schott, 2002; Pace-Schott and Hobson, 2002). Sleep spindles (7-14 hz) develop within the network of the nucleus reticularis thalami (NRT) and may play a role in neuronal plasticity (Hobson and Pace-Schott, 2002). They last approximatly 1-3 s and cause a refractory period of 3-20 s (McCormick and Bal, 1997; Hobson and Pace-Schott, 2002; Steriade, 2005).

1.2 The thalamocortical loop

The EEG oscillations described above are generated in the thalamus and cortex. Both are intimately linked by means of reciprocal projections. In doing so, they form the thalamocortical loop, which is an ideal system for synchronization of oscillations. It is illustrated in Figure 1.3. Glutamatergic cortical neurons project to the NRT and to thalamocortical relay neurons. Glutamatergic input to NRT neurons results in excitatory postsynaptic potentials (EPSPs). In the relatively hyperpolarized NRT neurons (negative to -65 mV), such EPSPs open T-type (also termed low voltage activated, LVA) Ca^{2+} channels, which results in an influx of Ca^{2+} (I_T) generating a low threshold Ca^{2+} potential termed low threshold spike (LTS). In turn, the LTS evoke high frequency Na^+/K^+ action potentials, which are typical for the burst mode and crown the LTS. These bursts cause GABAergic transmitter release onto thalamocortical relay cells, which elicits inhibitory postsynaptic potentials (IPSPs). When the IPSPs hyperpolarize thalamocortical relay cells beneath -65 mV, a hyperpolarization-activated cation current (I_h) is activated and will depolarize the membrane potential. This results in the generation of an LTS which is crowned by a burst of Na^+/K^+ action potentials (Fig. 1.4). Glutamatergic projections from the thalamocortical relay neurons will then feed back to the NRT and the cortex and the cycle starts again (McCormick and Pape, 1990; Steriade et al., 1993b; von Krosigk et al., 1993; McCormick and Bal, 1997; Steriade and Timofeev, 2003).

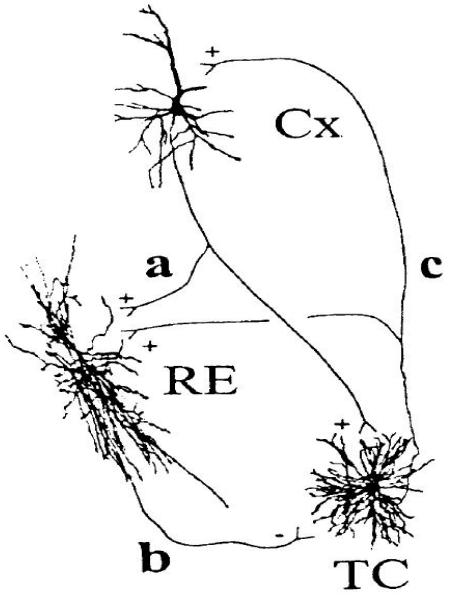

Fig. 1.3: The thalamocortical loop. Glutamatergic projections (a) from the cortex (Cx) terminate in the nucleus reticularis (RE, also NRT) and thalamocortical relay neurons (TC). GABAergic NRT neurons send axon collaterals (b) to TC neurons, which project back (c) to the NRT and to the cortex. Thus, a feedback loop is created which is able to generate oscillatory activity. Figure was taken from Steriade and Timofeev (2003).

The thalamocortical loop can only function in the described manner, when thalamic neurons are in a hyperpolarized state. During depolarization, when network activity converts from the oscillatory burst mode to the tonic transfer mode, the specific channel properties which underlie I_t inactivate the current which is only de-inactivated again through hyperpolarization. Thus LTS, and, therefore, burst discharges, are only possible when neurons are hyperpolarized. In NRT neurons a slightly different type of intrinsic mechanism has been described during depolarized states. In these neurons the voltage dependence of the LTS is more positive than in thalamocortical relay neurons. This allows them to produce LTS even at relatively depolarized membrane potentials (e.g. -65 mV). Thus during depolarization, the LTS is able to activate high-threshold Ca^{2+} currents (HVA), which increases the intracellular Ca^{2+} concentration above the threshold for activation of the Ca^{2+}-activated K^+ current. This K^+ current, in turn, causes an afterhyperpolarization. Its duration and amplitude influences the amplitude of the next LTS and enables the neuron to fire several burst discharges in sequence (see Fig. 1.4). Moreover the entry of Ca^{2+} into the cell activates a Ca^{2+}-activated nonselective cation current (I_{CAN}) which depolarizes the neurons and causes shunting inhibition (McCormick and Bal, 1997).

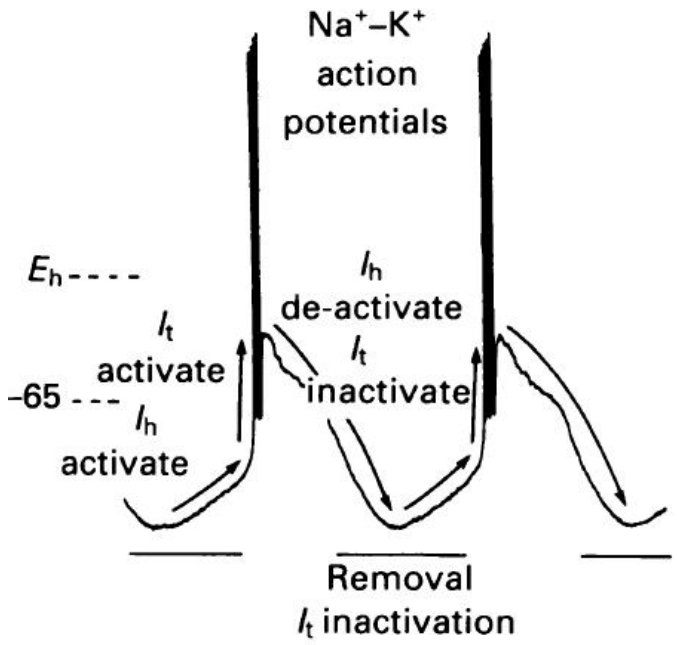

Fig. 1.4: Osillatory activity in thalamocortical relay cells. Activation of the low-threshold calcium current (I_t), produces an LTS which is crowned by Na^+-K^+ action potentials. The involved depolarization de-activates the hyperpolarization-activated cation current (I_h), which was active before the LTS. Inactivation of I_t repolarizes the membrane followed by a hyperpolarizing overshoot. The hyperpolarization activates I_h and de-inactivates I_t. The activated I_h depolarizes the membrane which results in activation of I_t and the cyle starts again. (From McComick and Pape, 1990).

1.3 Absence epilepsy

It becomes apparent from the description of the thalamocortical loop that the distinct intrinsic properties of the different types of neurons depend on their specific set of ion channels and receptors (e.g. LTS in thalamocortical relay neurons compared to LTS in NRT neurons). Thus, the oscillatory activity of the thalamocortical loop is very sensitive to changes in the involved ionic currents. Pathophysiological alterations within the oscillatory system can produce a switch from synchronized to hypersynchronized activity, which becomes noticeable in the EEG by the incidence of 3 Hz spike-and-wave discharges (SWD, Fig. 1.5) (Gloor, 1968; Avoli et al., 2001; Crunelli and Leresche, 2002).

Fig. 1.5: 3 Hz SWDs of childhood absence epilepsy. Video-EEG recording from an 8-year-old boy (Panayiotopoulos, 2008).

SWDs are a characteristic of absence epilepsy, which is a non-convulsive type of epilepsy of polygenic origin. It occurs predominantly during childhood, with its peak at an age of 6-7 years. Seizures, which are characterized by a loss of consciousness and may be accompanied by subtle movements of limbs and/or eye lids, occur many times each day (up to 200 per day in the juvenile form). However, around 70% of the patients show spontaneous remission, often during adolescence (Crunelli and Leresche, 2002).

1.3.1 The WAG/Rij model of absence epilepsy

Childhood absence epilepsy is one of the most prevalent epilepsy syndromes up to the age of 15 years. The incidence is about 1% (Blom et al., 1972). Many experimental models of epilepsy used in vitro preparations to explore seizure characteristics (as reviewed in Crunelli and Leresche, 2002). In comparison to an in vitro preparation, the present results were obtained from in vivo experiments in rats of the WAG/Rij strain. The advantage of in vivo studies is that the synaptic network connections which underlie SWDs stay intact, thereby allowing the study of temporal relationship between thalamic areas and cortical SWDs.

The WAG/Rij strain is a well established model for human absence epilepsy, since in humans and in rats a comparable relationship with the state of vigilance has been found. Nevertheless, there are differences in the ontogeny between man and rats and also in the frequency of SWDs. However, the behavioural traits during seizures show convincing similarities. Furthermore, many drugs have already been evaluated in the WAG/Rij model. It has been shown, that ethosuximide, valproate and trimethadione function as anti-absence drugs and suppress SWDs in the WAG/Rij rats. Because those drugs also suppress seizure activity in humans, the model predicts correctly the anti-absence profile of these drugs (reviewed in Coenen and van Lujtelaar, 2003). Another rodent model for absence epilepsy is the GAERS strain (Genetic Absence Epilepsy Rats from Strasbourg), which shows the same characteristics (Marescaux and Vergnes, 1995).

1.3.2 The putative role of thalamic networks to absence epilepsy

Previous studies showed that the thalamocortical loop, which generates oscillations during sleep, also produces absence seizures. As opposed to the sleep-rhythms, these oscillations show a dramatic increase in synchronization during SWDs. The seizure starts by a concerted interaction within the thalamocortical network. The initiation of this occurs in regions of the somatosensory cortex (Meeren et al., 2002). Cortical SWDs are the result of increased synaptic excitation via N-methyl-D-aspartic acid (NMDA) receptors, reduced GABAergic inhibition and an altered expression of hyperpolarization-activated cyclic nucleotide gated (HCN) channles (Van Luijtelaar et al. 2002). When cortical SWDs reach the NRT via corticofugal fibers, the NRT network answer with burst activity which is synchronized with the EEG-SWDs. This is due to two pathophysiological alterations. First, increased corticofugal activation can facilitate synchronization (Blumenfeld and Mc Cormick, 2000).
Second, the expression of a Ca^{2+}-channel subunit ($Ca_V3.2$) is increased in “epileptic” NRT neurons which results in higher amplitude of I_T and thus enhance synchronized burst activity (Tsakiridou et al., 1995; Talley et al., 2000). The GABAergic NRT neurons are reciprocally connected to the excitatory relay cells. As described above, relay cells produce LTS when activated by NRT neurons. During SWD, this LTS are synchronized with the spike-component of the SWDs. Because the LTS is transferred back to the NRT neurons and to the cortex, there are two possibilities of a restart of the described cycle (restart of the cycle in the NRT and/or in the hyperactive cortex).

In that process, pathophysiological alterations in relay cells are of importance. It was found, that in “epileptic” relay cells, the expression of the HCN1 isoform of the I_h is increased. This results in a reduced sensitivity of the pacemaker current I_h and therefore causes a prolonged rhythmic burst activity, which in turn enhances synchrony of thalamocortical activity towards seizure activity (Budde et al., 2005a).

1.4 Objectives of the dissertation

The intralaminar thalamus, which is located lateral to the mediodorsal nucleus of the thalamus, consists of four major nuclei, namely the parafascicular nucleus (Pf), the centromedial nucleus (CM), the centrolateral nucleus (CL), and the paracentral nucleus (PC). The intralaminar thalamic nuclei (ILTN) play a role in arousal and awareness, are an important component in the nociceptive system, and contribute to remote memory processing (Van der Werf et al., 2002; Lopez et al., 2009; Ren et al., 2009). Because most studies of SWDs focused on the NRT or on specific nuclei of the thalamus (for instance Pinault et al., 1998; Charpier et al., 1999; Steriade and Amzica, 2003), comparatively little is known about the role of ILTN in the generation of SWD. However, experiments in cats showed that SWD-like patterns can be evoked by stimulating the ILTN (Jasper and Droogleever-Fortuyn, 1947). From this finding it was hypothesized that the ILTN could function as the pacemakers of SWDs. In concordance, the ILTN exert a more powerful influence on cortical cells than other thalamocortical neurons, and thus have a strong effect on the thalamocortical loop (Steriade et al., 1993a).

It can be assumed that a pacemaker is active before the occurrence of SWDs, and thus leads oscillations. Indeed, unit recordings in the CL and PC demonstrated that neuronal activity is delayed with respect to the SWDs, which is not in support of such pacemaking function (Seidenbecher and Pape, 2001). However, intracellular recordings in vivo in neurons of the PC produced ambivalent results (Prof. Dr. Ali Gorji, by personal communication): the tonic activity of the depolarized state is suppressed during the peak component of the SWDs, whereas the burst activity of the hyperpolarized state is correlated to the spike component of the SWDs. Thus, activity of the depolarized state is unsupportive of a pacemaking function, whereas it is supported by the activity of the hyperpolarized state.

One caveat of intracellular recordings is that the recorded neuron is possibly influenced by leakage currents produced by the penetration of the cell membrane. Thus it is questionable, how precisely the depolarized or hyperpolarized membrane potential reflects the physiological state. In consideration of the ambiguous data, the main objective of the present study was to provide evidence for the pattern of activity and thus the putative role of ILTN as pacemakers for SWDs.

In a first set of experiments, unit recordings in PC neurons were performed to investigate their physiological firing pattern during SWDs. Unlike intracellular recordings, unit recordings can monitor neuronal activity without impaling the cell membrane. Thus, neuronal activity obtained from unit recordings avoids interference with the physiological state. Because GABAergic neurons in ILTN seem to play a role during SWDs (Seidenbecher and Pape, 1998), we tested the influence of $GABA_A$ and $GABA_B$ to neuronal activity during SWDs in a second set of experiments. This was achieved by microiontophoretic application of the $GABA_A$ receptor antagonist bicuculline and the $GABA_B$ receptor antagonist CGP 55845.

Finally, microstimulation experiments were performed to investigate the contribution of PC neurons to SWDs. Microstimulation experiments allow manipulation of the whole nucleus (in contrast to microiontophoresis experiments), which is a prerequisite to obtain changes in the EEG. Should the PC be the pacemaker of SWDs, stimulation of this nucleus would produce SWDs in the EEG. However, if neuronal activity in the PC has to be suppressed to allow occurrence of SWD, as indicated by activity during depolarized states, stimulation of that nucleus should result in suppression of SWDs.

All experiments were performed in vivo in Wistar albino Glaxo rats of Rijswijk (WAG/Rij), in which nonconvulsive SWDs occur spontaneously. This rat strain is a well established model of absence seizures in human patients and is, therefore, ideal to investigate the basic mechanisms of absence epilepsy (Coenen and Van Luijtelaar, 2003).

2. Material and Methods

2.1 Experimental setup

The electrophysiological principle was identical in all experiments, with the specific difference relating to the probe (unit recordings: tungsten electrode; microiontophoresis: three barrel glass electrode; microstimulation: bipolar wire in combination with a tungsten electrode). Depending on the probe used, neuronal activity was influenced in different ways. During microiontophoresis different charged molecules were applied to the recorded neuron by constant current, during microstimulation a direct current was used to manipulate neuronal cells. Neuronal signals were recorded as filed potentials from the surface of the exposed skull (electrocorticogram, ECoG) and as unit activity locally in the thalamus (Fig. 2.1).

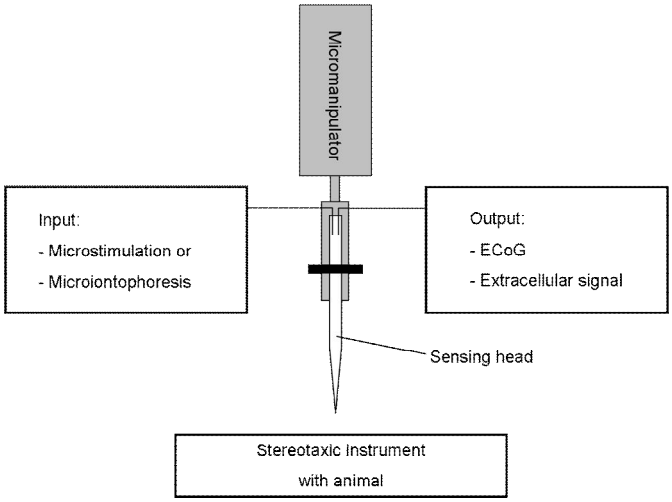

Fig. 2.1: Illustration of the signal path in the experiments. The probe was fixed to the micromanipulator which allowed movements in all three spatial dimensions and was used for targeting the brain area of interest. The input signal varied depending on the sensing head used, whereas the output signal was identical in all experiments.

The measured signals were amplified, filtered (DPA-2FX, npi electronic GmbH, Tamm, Germany) and fed to a connector board which was attached to an oscilloscope (HM507, Hameg Instruments GmbH, Mainhausen, Germany), an analogue to digital-converter (A/D-converter; CED 1401, Cambridge Electronic Design, Cambridge, United Kingdom), and a Neurocorder (Neurocorder DR-890, Cygnus Technology, Southport, North Carolina).

Signals from the A/D-converter were fed into a personal computer where they were monitored (Spike2 software, Cambridge Electronic Design, Cambridge, United Kingdom). The Neurocorder transformed the received signals into video-compatible data to allow storage of data on video-tape. To avoid influences of electric fields to the measured signals, the complete equipment was grounded to the signal-ground of the amplifier (Fig. 2.2).

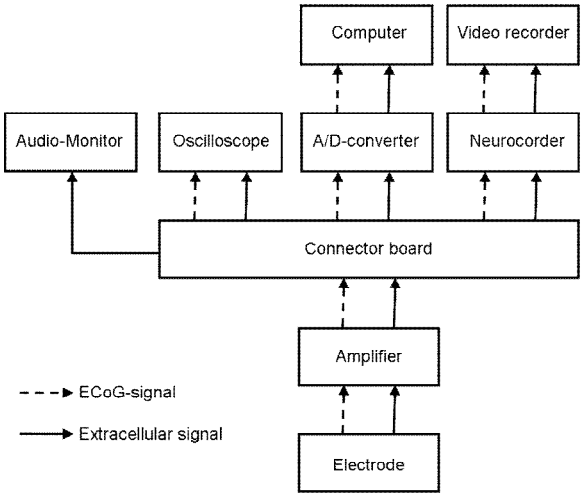

Fig. 2.2: Illustration of the signal path in the experiments. Recorded signals were amplified and connected to an audio-monitor, oscilloscope, A/D converter, and a Neurocorder. Data from the A/D converter and Neurocorder were fed into a computer and video recorder, respectively.

2.2 Preparation and monitoring of animals

Experiments were performed on 31 male rats of the WAG/Rij strain, aged between 150 and 300 days postnatal and a weighting of 250 to 350 g. All experimental procedures were approved by the legal authorities (Veterinäramt Münster (G57/2005)).

Following light anaesthesia with isoflurane (Forene, agent: 1-Chloro-2,2,2-trifluoroethyl-difluoromethylether, Abbott Laboratories Limited, Wiesbaden, Germany), the animal was deeply anesthetized by injecting pentobarbital (40 mg/kg) intraperitonal (i.p.). The animal was positioned in a stereotaxic instrument. Xylocain (Xylocain-Gel 2%, agent: lidocainhydrochloride, Astra Zeneca GmbH, Wedel, Germany) was applied to all pressure points. The eye bulbs were moistened (Bepanthen Augen- und Nasensalbe, Bayer, Leverkusen, Germany). Body temperature was monitored rectally and maintained at 37 °C with by a heating element (L/M-60, List Elecetronic, Darmstadt, Germany).

After verifying that the animal was deeply anaesthetized (loss of limb-withdrawal reflex), scissors were used to cut open the scalp of the animal. Bleeding was minimized by treating the tissue with 4% hydrogen peroxide (H_2O_2). After dissection of the cranial bone, H_2O_2 was used to visualize the fissures of lambda and bregma. After that, the stereotaxic instrument was adjusted in such a way that lamda and bregma were positioned in the same horizontal plane. The micromanipulator, which could be moved precisely in all three spatial dimensions by using its readout for coordinates, was used to control their positions. From the bregma, the positions of the later drillholes, for reaching the CL and PC with the sensing head, were marked with ink (bregma (B): -2.8 mm, lateral (L): ±1.315 mm). The cranial bone was gently drilled to permanently mark the positions.

For bilateral epidural ECoG recording holes were drilled over the prefrontal region (B: +1.8-2.2 mm, L: ±3.6-3.8 mm). A silver wire (AGW1030, World Precision Instruments, Berlin, Germany), which was melted to a small sphere at one end (diameter: ~1 mm), was used as an ECoG-electrode. Two such electrodes were placed onto the dura with the surface of the sphere and fixed to the skull with dental acrylic cement (Paladur, Heraeus Kulzer GmbH, Hanau, Germany). The reference-electrode was produced and fixed in a similar way (intraaural (I): -1.0-1.5 mm, L: 3.4-3.6 mm) (Fig. 2.3).

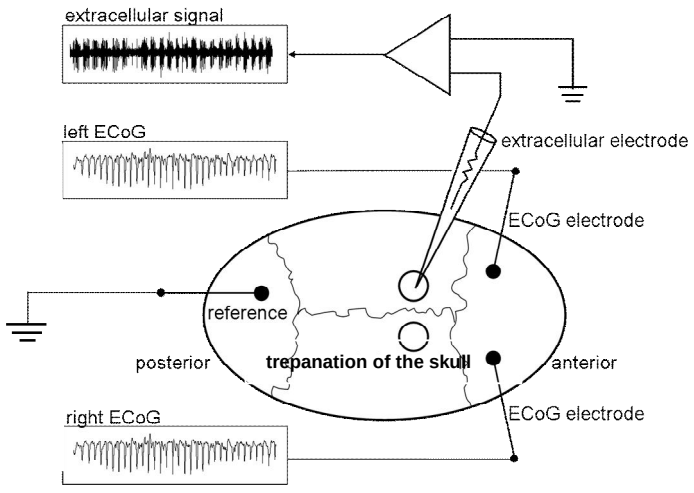

Fig. 2.3: Illustration of the experimental setup. Prepared rat skull. To measure the ECoG, three Ag-ECoG-electrodes were placed above the dura: two active electrodes over the somatosensory cortex and the reference-electrode over the cerebellum. Two additional holes were drilled into the skull (B: -2.8mm, L: ±1.315mm) to obtain extracellular recordings in the PC and CL.

In a final step the predrilled holes were finished. The dura was removed gently to enable penetration of the brain without damaging the sensitive electrode tip. Artificial cerebrospinal fluid (ACSF) was applied to the cortex to prevent drying out. ACSF contained 125 mM NaCl, 3 mM KCl, 0.8 mM $MgCl_2$+$6H_20$, 0.5 mM Na_2HPO_4+$2H_2O$ and 1.1 mM $CaCl_2$.

Recordings were performed under neurolept anaesthesia through Fentanyl (Fentanyl, agent: Fentanylcitrate, Janssen-Cilag, Neuss, Germany) and Droperidol (Xomolix, agent: droperidol, ProStrakan, Galashiels, UK). Both drugs were administered intraperitonal (i.p.) at 15-20 min intervals, as required to maintain a light neurolept-anaesthesia (mean doses: 0.18 (mg/kg)/h i.p. Fentanylcitrat and 3.17 (mg/kg)/h i.p. Droperidol. Anaesthethic conditions were continuously monitored through the ECoG and the limb withdrawl response. At any sign of stress to the animal, anaesthetic doses were additionally administered.

2.3 Electrophysiological measurements

Unit recordings and microstimulation were performed in the CL and PC, microiontophoretic data were obtained from the PC. The ECoG was recorded in all experiments.

2.3.1 Recording of ECoG

ECoG electrodes were connected to an amplifier. Signals were amplified and filtered (bandpass 3-30 Hz).

2.3.2 Unit recordings

Unit activity was measured with custom-made tungsten electrodes (TM33A10, resistance: 1 MΩ, Microelectrode Tungsten, World Precision Instruments, Berlin, Germany). They were mounted on a Plexiglas holder (length: 35 mm, diameter: 3 mm) and lowered into the brain with a micromanipulator through aid of a nanostepper (David Kopf Instr., Tujunga CA, USA) (Fig. 2.4).

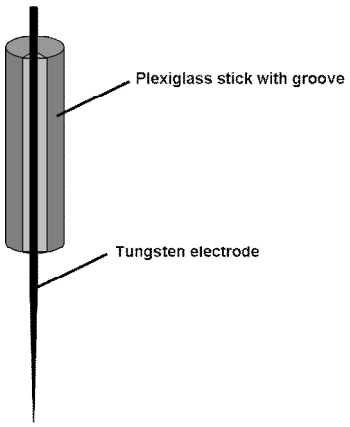

Fig. 2.4: Illustration of the sensing head for unit-recordings.

Electrode position was monitored by the micromanipulators control unit relative to the electrodes entry position. The electrode was moved in 5 µm steps through cortex and hippocampus to the thalamus. Before entering the target area, a waiting period of 10 min ensured that potentially deformed brain tissue recovered to its original position. The electrode was moved in 2 µm steps through the thalamus until the CL or PC was reached. Recorded unit activity was amplified and filtered (bandpass 0.3-3 kHz). At the end of a recording session, the position of the electrode tip was marked by a small electrolytic lesion through current pulses (pulse duration: 10 s, amplitude: 20-50 µA, number of pulses: 2-6 with alternating negative and positive current) which were applied via a stimulus isolator (Stimulus Isolator A365, World Precision Instruments, Berlin, Germany).

2.3.3 Microiontophoresis

2.3.3.1 Fabrication of the electrode

Recording of unit activity and drug application were done using three-barrel borosilicate glass capillaries (3B120F-6, World Precision Instruments, Berlin, Germany). The three-barrel capillary was mounted into a vertical puller (L/M-3P-A, List Medical, ePS, Siegen, Germany), heated locally by a heating coil and pulled lengthwise to a defined length. In a second run, the top and bottom part of the capillary were separated with reduced heating settings, which resulted in a very fine tip (diameter below 1µm).

In an additional step, the tip was broken back by moving it against a glass-stick under microscopic control (Narashige Scientific Instrument Lab, Tokyo, Japan). Electrodes which were used for recordings had a tip diameter of ~3 µm. It was ensured, that the tips had clean brims (Abb. 2.5).

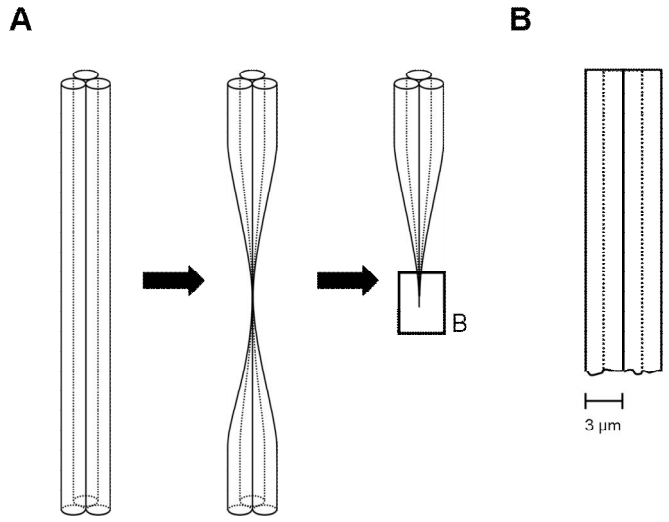

Fig. 2.5: Production of the microiontophoresis electrode. **A)** In a first step, the capillary was pulled lengthwise under local action of heat. With a second pull, the top and bottom of the capillary were separated, which resulted in a fine tip. **B)** The fine tip was broken under microscopic control to obtain a tip with a final diameter of ~3 µm.

A fibre glass cannula (World Precision Instruments, Micro-Fil, MF286-5) was used to fill the barrels of the electrode with different solutions. The barrel which recorded unit activity was filled with 0.5 M sodium acetate. The second barrel contained 165 mM NaCl and either 5 mM of the $GABA_A$ antagonist bicuculline methiodide (Fluka, Cat No. 14343, Sigma-Aldrich, Munich, Germany) or 5 mM of the $GABA_B$ antagonist CGP 55845 (Tocris, Cat No. 1248, Biozol GmbH, Eching, Germany). Injections of drugs were controlled by ejection- and retention-currents through a Neurophore BH-2 (Medical Systems Corporation, Greenvale, NY, USA). Because these currents could apply charge carriers to the tissue, which could influence the measured signal, a third barrel was filled with 0.5 M sodium acetate to balance these currents. In addition, this barrel contained 4% Chicago Sky Blue (Sigma, Cat No. C8679-25G, Sigma-Aldrich, Munich, Germany), which was needed to mark the recording site at the end of the experiment. To make sure that the drugs were ionised in 165 mM NaCl (ejection with current), the solution was adjusted with 1 M hydrochloric acid to pH 3.4-3.6. A Ag/AgCl wire connected each barrel to the Neurophore control unit. Leakage currents between the barrels were prevented by sealing each barrel with sealing wax (Deiberit 502, Bad Sachsa, Germany). Resistances (measured at 1 kHz) were between 10 MΩ and 30 MΩ and were routinely checked during experiments.

2.3.3.2 Microiontophoretic application

Before penetrating the brain with the electrode, the retention current was set to -15 nA. This causes a redistribution of the charge carrier, which was compensated automatically by the microiontophoretic device. Measured signals were amplified and filtered (bandpass 0.3-3 kHz). All substances were applied microiontophoretically (20±50 nA injection current; retaining currents -15 nA) for 1 min after a 1 min preapplication control, followed by a 1 min postapplication period. The number of drug applications depended on how long a stable neuronal response was obtained.
Furthermore, it was verified, that the occurrence of SWDs was constant over the application and recovery periods. At the end of the experiment, the recording site was marked with Chicago Sky Blue by connecting the corresponding barrel to the stimulus isolator. The dye was ejected for 10-15 min with a current of -0.2 mA.

2.3.4 Microstimulation

For local electrical microstimulation within CL and PC, a bipolar electrode was used. Non-insulated tips protruded about 5µm from the insulated shaft. One stimulation electrode and one tungsten recording electrode were inserted into a Plexiglas capillary under microscopic control, and fixed by acrylic glue with the recording electrode protruding 50-150 µm from the stimulation electrode, and both protruding >300 µm from the orifice of the capillary (Fig. 2.6).

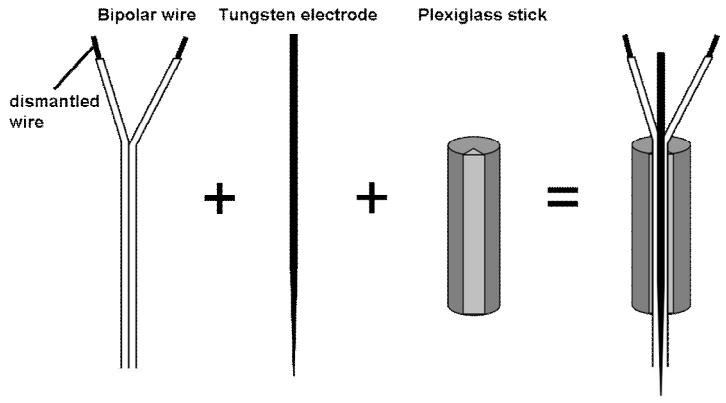

Fig. 2.6: Production of the microstimulation electrode.

Microstimulation was achieved via the stimulus isolator connected to a control unit (Master-8, A.M.P.I., Cygnus Technology, Southport, North Carolina). Stimulus pulses were generated at 7 Hz or 40 Hz (amplitude: 0.4 mA, pulse duration: 2-4 s). During the stimulation period it was verified, that the occurrence of SWDs was constant over the application and recovery periods.

2.4 Data analysis

2.4.1 Unit recordings

The measured data were analysed with the Spike2 Software (Cambridge Electronic Design, UK). To evaluate the correlation between unit activities and the ECoG-SWDs, SWDs and unit activity of the same hemisphere were related to each other. Unit activity was discriminated from noise using the level-time function of Spike2. Activity, which exceeded the baseline noise by more than threefold, was taken for analysis. The same level-time function was used to mark the peaks of the spike components of SWDs, which were used as a trigger for analysis. Unit activity was analysed in a time period 60 ms before and 60 ms after a trigger and was illustrated as histogram (Peri-Stimulus-Time-Histogram, PST histogram). A detailed explanation for the generation of a PST histogram is given in figure 2.7. For each recording a PST histogram was created, which was based on 300 triggers. PST histograms of all recordings from the same brain region were averaged at the end. The average numbers of cellular discharges for each SWD were calculated from the number of spikes in the PST histograms divided by the number of SWDs.

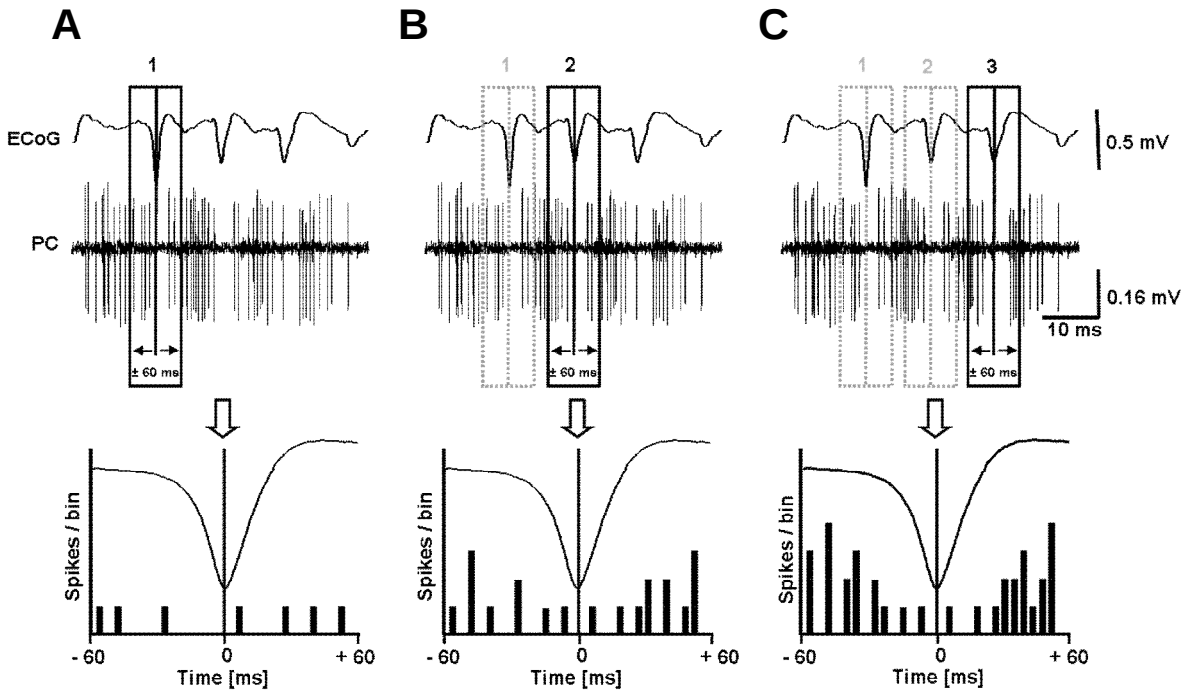

Fig. 2.7: Generation of a Peri-Stimulus-Time-Histogram. **A)** The spike peaks of ECoG-SWDs were detected by the Spike2 software. In the following procedure, they were used as trigger for analysing unit activity. Unit activity was evaluated in between a defined time frame (120 ms), which was set with respect to the trigger (60 ms before and 60 ms after the trigger). The time frame was divided into 120 bins, thus each bin contained a time period of 1 ms. The Spike2 software counted the number of action potentials per bin. The obtained data were visualised by plotting the number of action potentials against the time period of the time frame. **B) and C)** After the neuronal activity within one time frame was analysed, the time frame was moved to the next trigger and the procedure was repeated. Neuronal activity of all analysed time frames was summed.

2.4.2 Microiontophoresis

For microiontophoretic application of a substance, cycles of ejection and retention currents were systematically altered to achieve stable effects. PST histograms were calculated for time periods immediately before, at the end, and 30s after an ejection cycle. For each time period, unit activity was collected from 75 SWD-triggered sequences (as described in section 2.4.1), and cycles were averaged from different unit recordings (Fig. 2.8).

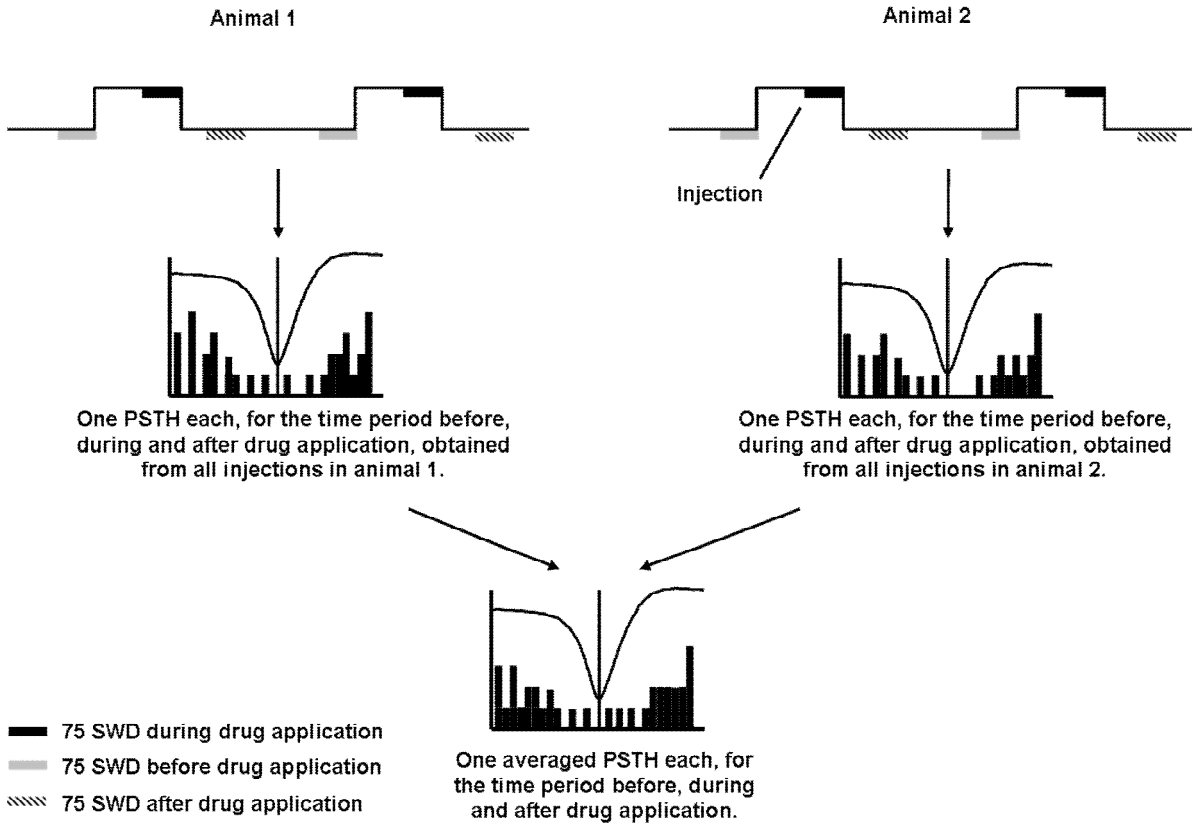

Fig. 2.8: Generation of the PST histogram in the microiontophoresis experiments (for details see Fig. 2.7). An example of two different recordings (Animal 1 and Animal 2) with two drug injections each is shown. Each injection was divided into three different time periods (before, during, and after drug application). A PST histogram for each time period and recording was created. In a final step, the PST histograms of all recordings were averaged. In the shown example, the final PST histogram included the information of two recordings (n = 2) with each recording containing two cycles of drug injections. Therefore, the average number of cycles in the final PST histogram is c = 2.

Unit activity and SWDs were discriminated from noise using the level-time function of Spike2. Unit activity, which exceeded the baseline noise by more than twofold, was analysed. SWDs, which exceeded the baseline noise by more than threefold were used as trigger. The software package Spike2 was used for data analysis.

2.4.3 Microstimulation

The number of SWDs recorded in the ECoG were compared in a time window 20 s before and 25 s after microstimulation. For that purpose, the time window was divided into 5 s intervals and the number of SWDs in each interval was counted. The numbers of SWDs for each interval were averaged for all recordings.

2.4.4 Statistics

Data were statistically analysed using Student's t-test for paired observations, and P-values <0.05 were considered to indicate significant differences. Averaged data are presented as mean ± standard error of the mean (SEM). The Wilcoxon signed rank test was chosen, as required for a non-Gaussian distribution, as specified in the results section.

2.4.5 Histology

Upon completion of the experiments, the animals were sacrificed by an overdose of pentobarbital (150 mg/kg, i.p.) and decapitated. The brains were rapidly removed and transferred into 4% phosphate-buffered paraformaldehyde (pH 7.4) which contained 20% sucrose. Brains were kept in this solution for at least 24 h. Afterwards, brains were sliced with a freezing-microtome (Frigomobil, Leica, Bensheim, Germany) into 50 µm coronal slices. Slices were washed for 2 h in phosphate-buffered saline (PBS; containing (in mM): 8.3 Na_2HPO_4, 3 KH_2PO_4, 123 NaCl) and were placed on a microscope slide thereafter, where they were air dried for 24 h. The marked recordings sites were identified after counter staining the coronal slices with Cresyl Violet (Tab. 2.1). Finally, counter stained slices were covered with DePeX (SERVA Electrophoresis GmbH, Heidelberg, Germany).

Tab. 2.1

Step	Solution	Application time [min]	Step	Solution	Application time [min]
1	100% Ethanol	3	**8**	70% Ethanol	3
2	100% Ethanol	3			
			9	Aqua dest.	3
3	Isopropanol	3	**10**	Cresyl Violet	3-4
			11	Aqua dest.	3
4	Roti-Histol	3			
5	Roti-Histol	3	**12**	70% Ethanlol	1
			13	96% Ethanol	1
6	Isopropanol	3			
			14	Isopropanol	1
7	100% Ethanol	3	**15**	Roti-Histol	1

Data from recordings were only included for analysis in the present study when recording sites had been histologically verified (Fig. 2.9).

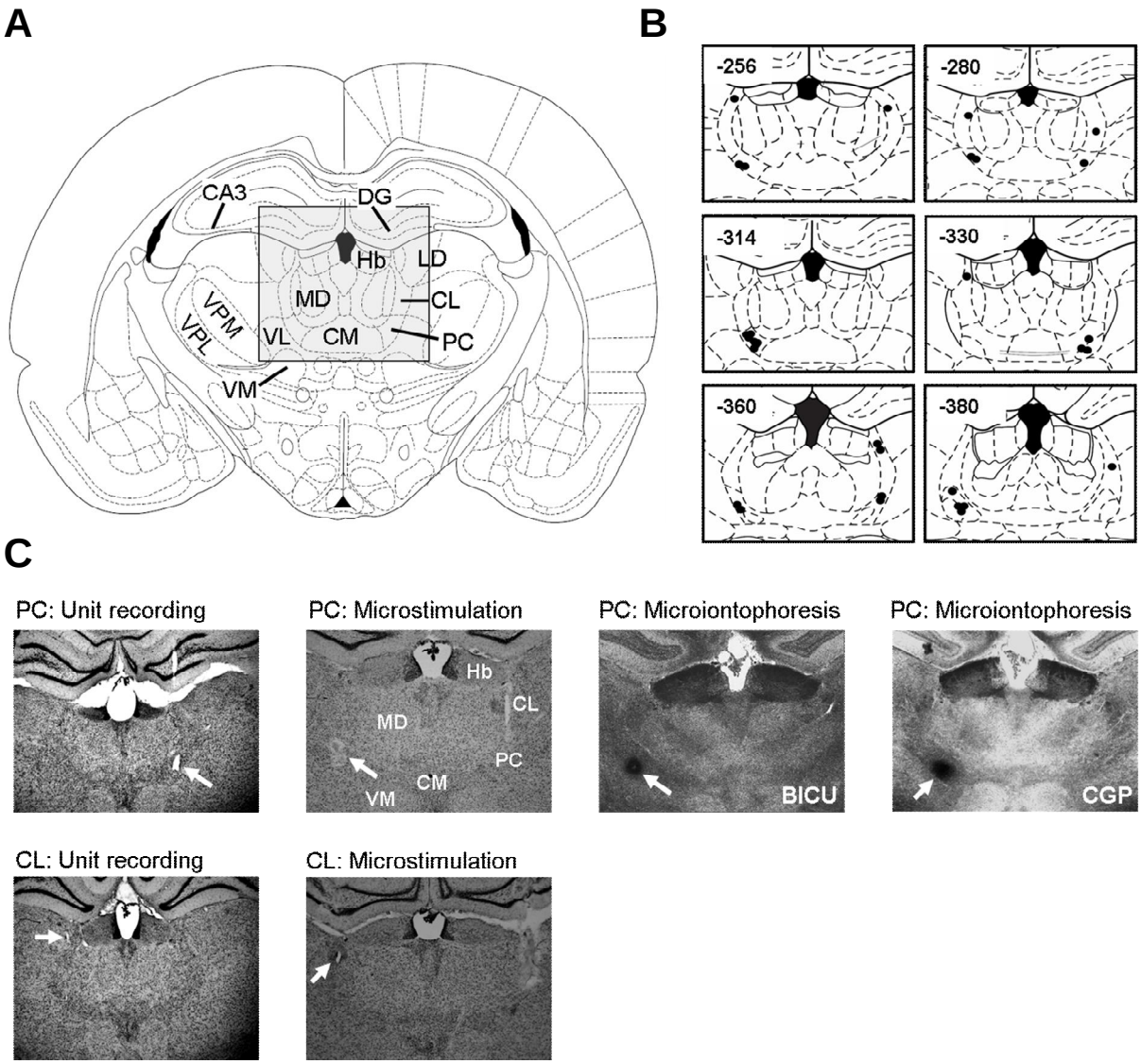

Fig. 2.9: Histological verification of recording sites. **A)** Drawing of a coronal brain slice, including PC and CL (Bregma: -330mm). The grey shaded area is shown in B). **B)** Verification of the recording sites. Each black dot indicates the recording site of one experiment. The recording sites of unit recording, microiontophoresis and microstimulation experiments are plotted. The numbers at the top left indicate anteroposterior distance from bregma. **C)** Original coronal sections. The white arrows indicate the electrolytic lesion marking the electrode tip and thus the recording sites. CA3: field CA3 of hippocampus; CL: centrolateral thalamic nucleus; CM: centromedial thalamic nucleus; DG: dentate gyrus; Hb: habenular nucleus; LD: laterodorsal thalamic nucleus; PC: paracentral thalamic nucleus; VM: ventromedial thalamic nucleus; VPL: ventral posterolateral thalamic nucleus; VPM: ventral posteromedial thalamic nucleus (Coronal drawings and abbreviations are adapted from Paxinos and Watson, 1998).

3. Results

3.1 Spike and Wave discharges

Under neurolept anaesthesia, all animals of the WAG/Rij strain developed bilaterally synchronized SWDs at 5-10 Hz (as observed on the epidural ECoG), which started and ended abruptly on a normal background pattern. The peak-to-peak amplitude of the SWDs was between 350 and 1200 μV. On average, the SWDs lasted 5 ± 0.3 s (number of analysed SWDs: n=80) and had a frequency in the range of 5-10 Hz, analysed by fast Fourier transformation of the ECoG. It was often observed, that the vibrissae and facial muscle twitched simultaneously and with roughly the same frequency as SWDs (Vergnes et al., 1982; Seidenbecher et al., 1998).

3.2 Unit recordings in the paracentral and centrolateral nucleus

Unit acticity during SWDs in the PC was analysed in 10 WAG/Rij rats. During SWDs, neurons in the PC showed a very prominent firing characteristic: tonic activity was interrupted during the peak components of the SWDs (Fig. 3.1). This interruption began 8.3 ± 2.2 ms (number of analysed animals: n=10) before the peak component of the SWDs and ended 28 ± 6 ms (number of analysed animals n=10) after it (an activity of 5 Spikes/bin was chosen as threshold). The maximimum activity was reached in average 56 ± 1 ms (number of analysed animals: n=10) after the peak components of the SWDs and decreased 49 ± 4 ms (number of analysed animals: n=10) before the peak components of the SWDs (Fig. 3.2 A).

Recording of unit activities during seizure-free episodes revealed tonic activity with an average frequency of 35 ± 3 Hz (number of analysed unit activities: n=18) (Fig. 3.1). The mean interspike interval was 33 ± 3 ms (number of analysed unit activities: n=18). During SWDs the frequency increased to 183 ± 10 Hz (number of analysed unit activities: n=88), and the interspike interval shortened to 7 ± 1 ms (number of analysed unit activities: n=88). In contrast to unit activity in the PC, neurons of the CL showed burst like discharges that were highly correlated to the SWDs (Fig. 3.1).

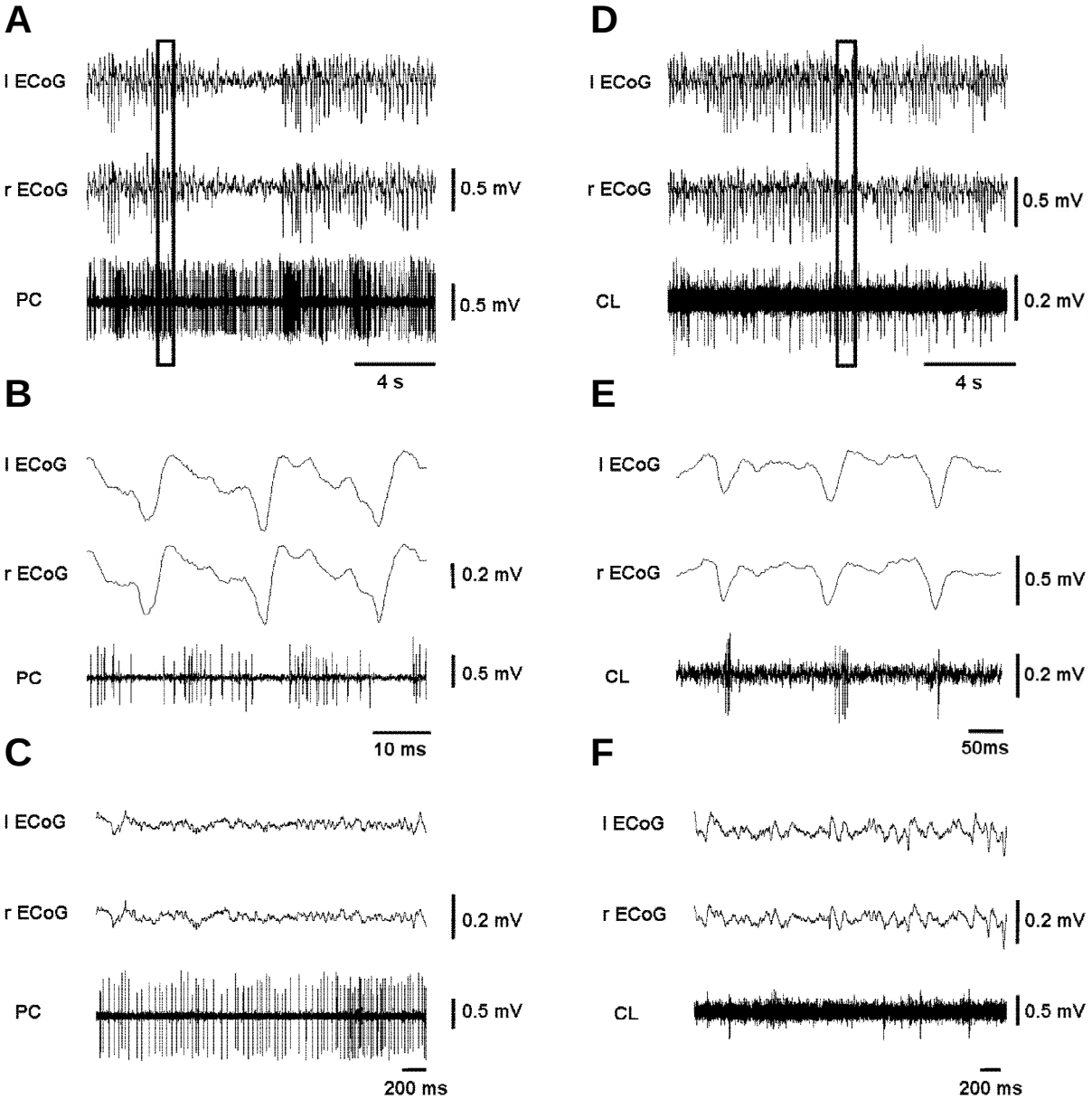

Fig. 3.1: Example traces of discharge patterns in intralaminar thalamic neurons. Upper and middle traces in each panel represent ECoG recordings, lower traces are unit recordings in the PC and CL, respectively. **A)** Overview of SWDs and corresponding unit activity in the PC. The marked area is shown in B) at an expanded timescale. **B)** The tonic firing pattern was interrupted during the peak components of SWDs. **C)** In SWD-free periods tonic activity was not suppressed. **D)** Overview of SWDs and corresponding unit activity in the CL. The marked area is shown in E) at an expanded timescale. **E)** During SWDs, unit activity in the CL showed burst-like discharges which were delayed with respect to the peak component of the SWDs. **F)** In SWD-free periods, burst like activity in the CL was reduced and appeared at random.

These discharges appeared during the rising phase of the wave component of the spike and wave complex, which was previously shown for CL neurons in GAERS rats (Seidenbecher and Pape , 2001). In comparison, neuronal activity in the ventrobasal complex and NRT is related to the spike component of the SWDs (Inoue et al., 1993; Seidenbecher et al., 1998). CL neurons showed maximum of activity 11 ± 3 ms (number of analysed animals: n=3) after the peak component of the SWD (Fig. 3.2 B). Burst like discharges had a frequency of 342 ± 18 Hz (n=51) with an interspike interval of 4 ± 0.2 ms (n=51). On average, burst like discharges lasted 16 ± 2 ms (n=51) and consisted of 5 ± 0.3 action potentials (n=51). During seizure-free episodes, unit activity appeared at random. These data are in accordance to previously published data (Seidenbecher and Pape, 2001).

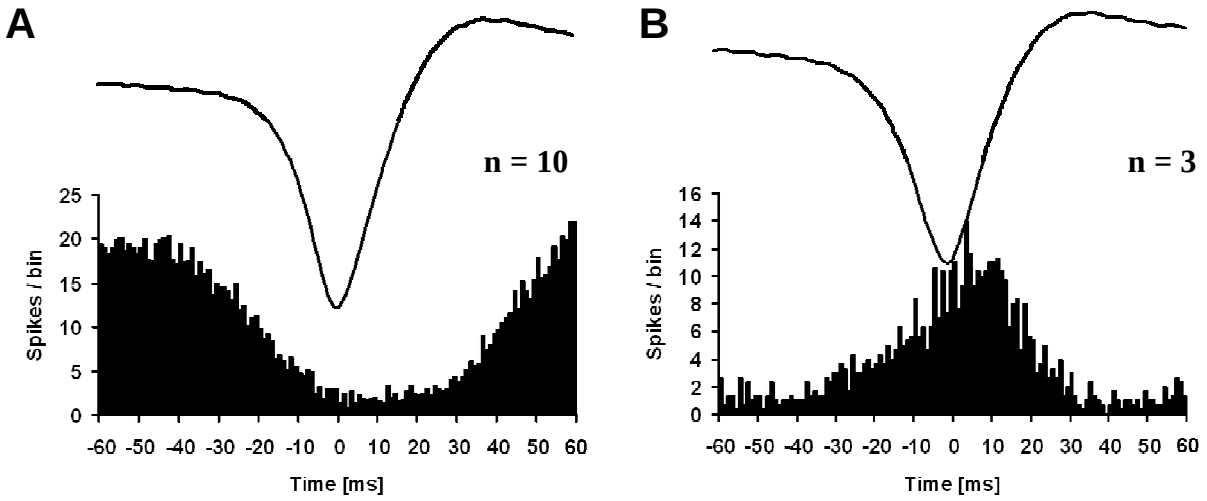

Fig. 3.2: Temporal relationship between SWDs and associated cellular activities. PST histogram of unit activity (bin width 1 ms) triggered by the spike component of the SWD on the ECoG demonstrate: **A)** Unit activity in the paracentral nucleus, which was interrupted during the spike component. **B)** Unit activity in the centrolateral nucleus, which was delayed with respect to the spike component in the ECoG. 300 SWDs per animal have been averaged for each PST histogram (n, number of neurons).

In summary, tonic unit activity in the PC was interrupted during the peak component of the SWDs, whereas unit activity in the CL was delayed with respect to the peak component of SWDs. In seizure-free periods, burst like discharges of CL neurons appeared at random. With respect to the findings obtained for intracellular recordings, it can be suggested that CL and PC neurons have different physiological firing behaviours: CL neurons always showed burst like discharges, PC neurons always fired in a tonic mode.

3.3 Microiontophoresis

In view of previous results of suggesting an involvement of GABAergic mechanisms in SWD-related discharges (Seidenbecher and Pape, 1998), the effects of microiontophoretic application of $GABA_A$ receptor antagonists were tested in the present study.

3.3.1 Effects of bicuculline on SWD-related firing

Microiontophoretic application of the $GABA_A$ receptor antagonist bicuculline caused a significant increase in SWD related unit activity (number of animals: n= 4, number of drug applications: n=13). Thus, application of bicuculline interfered with the SWD-related inhibition, in that discharges were generated during SWDs particulary at early phases. This disinhibitory effect resulted in a prolonged duration of SWD-correlated unit activity from 36 ± 2 ms to 63 ± 5 ms (number of analysed SWD: n = 217) ($p<0.0001$) and caused an increase in the number of action potentials per SWD from 4 ± 0.2 to 9 ± 0.6 (number of analysed SWD: n=217) ($p<0.0001$). In other words, during bicuculline application, SWD-correlated unit activity was suppressed 27 ms later (63 ms - 36 ms=27 ms) compared to unit activity in bicuculline free periods. As a consequence, additional action potentials could be generated during those 27 ms, which results in the described increase in the numbers of action potentials per SWD. Because of the prolonged duration of the unit activity (during bicuculline application), the action potential frequency increased only slightly but significantly from 165 ± 11 Hz to 171 ± 7 Hz (number of analysed SWD: n = 217) ($p = 0.012$) when bicuculline was applicated. Statistical analysis is based on the Wilcoxon signed rank test.

The prolonged unit activity of PC neurons under bicuculline is illustrated in Figure 3.3 (note areas of interest marked by dashed lines in panel A and B). Moreover, PST histograms calculated for periods before, after and during bicuculline application, showed that unit activity was not increased uniformly over the analysed time range. Unit activity increased during the early part of the SWDs (-60 ms to 0 ms), and interestingly, during the first 20 ms of the late phase of the SWDs (0 ms to +60 ms).

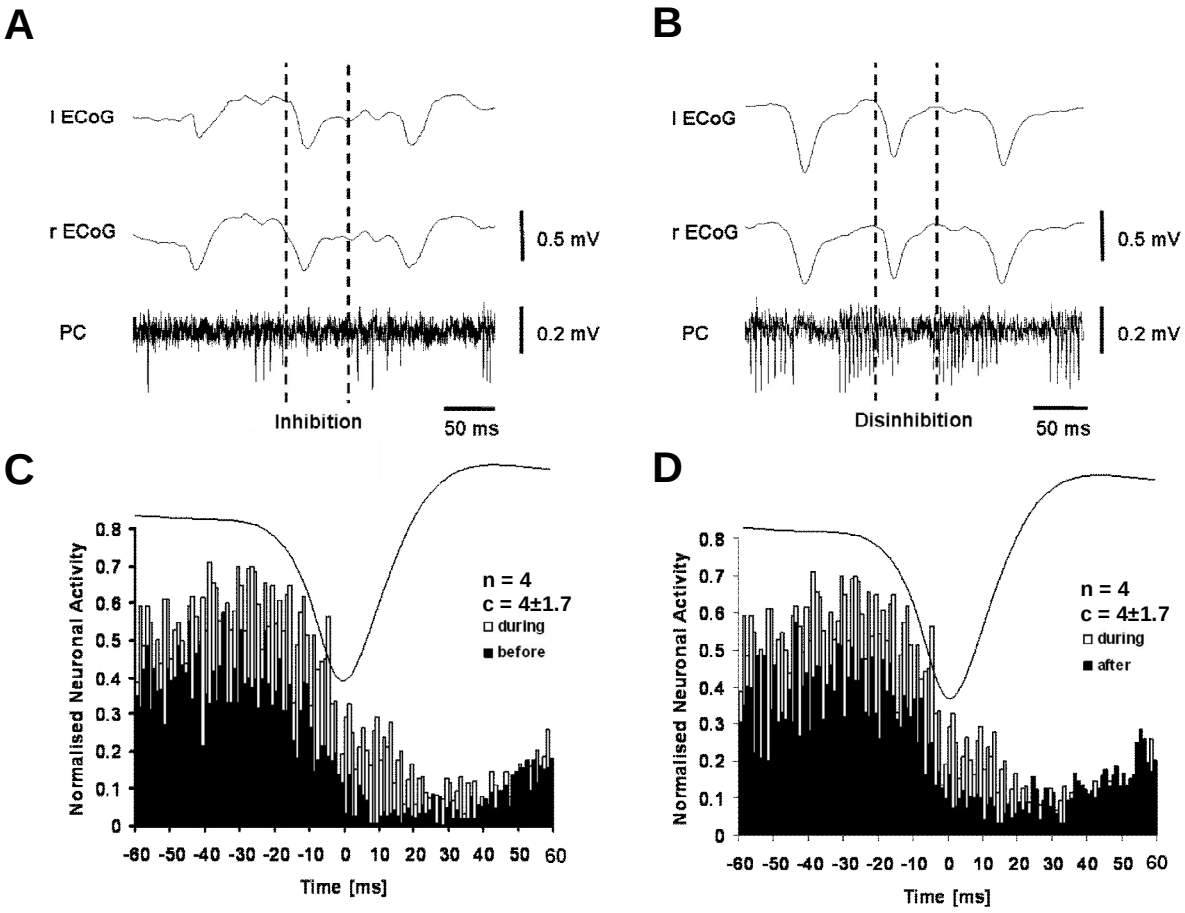

Fig. 3.3: Effects of microiontophoretic application of the $GABA_A$ receptor antagonist bicuculline on SWD-related unit activity in the PC. **A) + B)** Upper and middle traces represent ECoG recordings, the lower traces are unit recordings in the PC. Dashed lines indicate area of interest for easier comparison. During the control period (before application of bicuculline) unit activity in the PC was inhibited when SWDs were at peak component **(A)**. Application of bicuculline caused increased and prolonged unit activity in the PC during the early component of the SWDs **(B)**. **C)** PST histogram of unit-activity in the PC before (black bars) and during (white bars) application of bicuculline (bin width 1 ms). During application of bicuculline, SWDs did not inhibit unit activity by as much as in bicuculline free periods (note increased activity between 0 ms and 20 ms). **D)** PST histogram of unit-activity in the PC during (white bars) and after (black bars) application of bicuculline (bin width 1 ms) shows that the effect of bicuculline was fully reversible. n, number of neurons. c, number of cycles per neuron. Each cycle contained 75 SWDs (see methods for details).

These results indicate a disinhibitory effect of bicuculline at early phases of the SWD (Fig. 3.3).

Unit activity before, during, and after bicuculline application was investigated in more detail by analysing three intervals each for the early and late phase of the SWDs. Such an interval contained a time period of 20 ms. Using a two tailed paired Student's t-test, differences in unit activity before, during, and after bicuculline application were explored for each interval (Fig. 3.4).

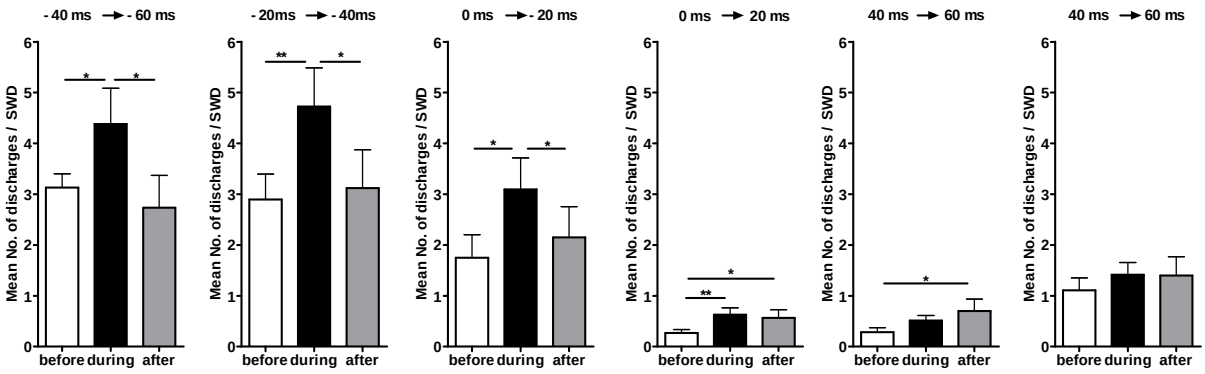

Fig. 3.4: Average number (mean ± SEM) of unit discharges in the PC associated with one SWD on the ECoG. Each diagram shows unit discharges before, during, and after bicuculline application. At the top of each diagram, the analysed interval with respect to the SWD is given. Negative values indicate intervals before, positive values indicate intervals after the peak component of a SWD. Data were obtained from PST histograms, averaged from recordings in 4 neurons. Number of cycles: 4 ± 1.7. Each cycle contained 75 SWDs.

Each interval in the early phase of the SWD yielded significant differences between unit activity before and during bicuculline application and between unit activiy during and after bicuculline application (-40 ms → -60 ms: before vs. during: $p = 0.026$, during vs. after: $p = 0.011$; -20 ms → -40 ms: before vs. during: $p = 0.005$, during vs. after: $p = 0.011$; 0 ms → -20 ms: before vs. during: $p = 0.019$, during vs. after: $p = 0.044$). In the late phase of the SWD there were significant differences in the interval from 0 ms to 20 ms (before vs. during: $p = 0.005$, before vs. after: $p = 0.049$) and in the interval from 20 ms to 40 ms (before vs. after: $p = 0.028$).

In summary, unit activity of PC neurons increased in the presence of bicuculline in the early phase and in the first interval of the late phase of SWDs. This effect was largly reversible within 30 s after cessation of microiontophoretic application. Increased activity was mostly due to a prolonged duration of unit activity, whereas frequency of unit discharges increased only slightly. Thus, the inhibitory effect of SWDs to the unit activity in PC neurons seemed to be less effective when bicuculline was applied to these neurons. Moreover it was tested, whether application of bicuculline in SWD-free episodes had an effect on unit activity. Therefore, time periods one second before the start of SWDs were analysed in episodes with and without bicuculline application. The time periods lasted two seconds. However, differences observed just failed to reach significance ($p = 0.0552$, not shown).

3.3.2 Effects of CGP on SWD-related firing

The effect of $GABA_B$ receptors to unit activity in PC neurons was tested by applying the $GABA_B$ receptor antagonist CGP 55845 (number of animals: n=4, number of drug applications: n=12). This increased the activity of PC neurons as assessed by unit recordings (Fig. 3.5). But in contrast to bicuculline application, CGP application did not interfere with the SWD-related inhibition. This means, that the duration of unit activity was unchanged during CGP application (before application: 30 ± 2 ms, during application: 32 ± 2 ms, number of analysed SWD: n = 124, p = 0.294). In other words, the duration of the SWD-correlated inhibition of unit activity did not change significantly during application of CGP. Thus, the increasing effect of CGP 55845 was due to an increase in action potential frequency (from 158 ± 9 Hz to 209 ± 10 Hz (number of analysed SWD: n = 124, p = 0.0002). The number of action potentials during one SWD changed from 3 ± 0.12 discharges before to 5 ± 0.25 discharges during CGP application (number of analysed SWD: n = 124, $p<0.0001$). Note that given p-values are based on the Wilcoxon signed rank test.

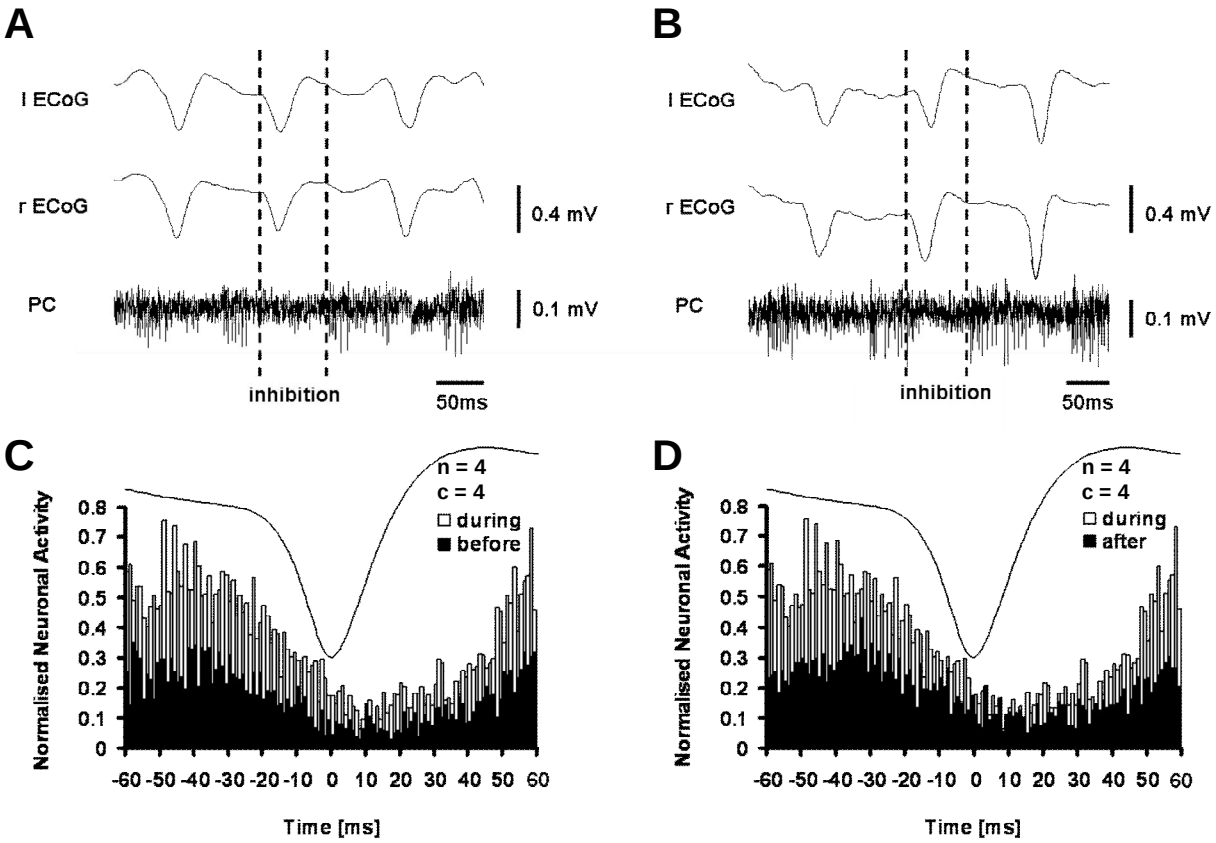

Fig. 3.5: Effects of microiontophoretic application of the $GABA_B$ receptor antagonist CGP on SWD-related unit activity in the PC. **A) + B)** Upper and middle traces represent ECoG recordings, the lower traces are unit recordings in the PC. Dashed lines indicate area of interest for easier comparison. During the control period (before application of CGP) unit activity in the PC was inhibited when SWDs were at peak component **(A)**. Application of CGP caused increased unit activity in the PC during the early and the late component of the SWDs **(B)**. **C)** PST histogram of unit-activity in the PC before (black bars) and during (white bars) application of CGP (bin width 1 ms). Unit activity was increased before and after the peak component of SWDs. **D)** PST histogram of unit-activity in the PC during (white bars) and after (black bars) application of CGP (bin width 1 ms) shows that the effect of CGP was reversible. n, number of neurons. In each neuron, number of cycles (c) was 4. Each cycle contained 75 SWDs.

Because the duration of unit activity was not prolonged under CGP 55845, it can be reasoned that SWDs interrupted the tonic activity of PC neurons as early as without application of CGP 55845. Figure 3.5 shows an example trace (compare the regions of interest indicated by the dashed lines in panel A and B). PST histograms calculated for time periods before, during, and after application of CGP 55845 revealed that unit activity increased during the early phase of the SWDs and, unlike bicuculline, also increased during the late phase of SWDs. As described above, unit activity was investigated in more detail by analysing several intervals of the early and late phase of SWDs (Fig. 3.6).

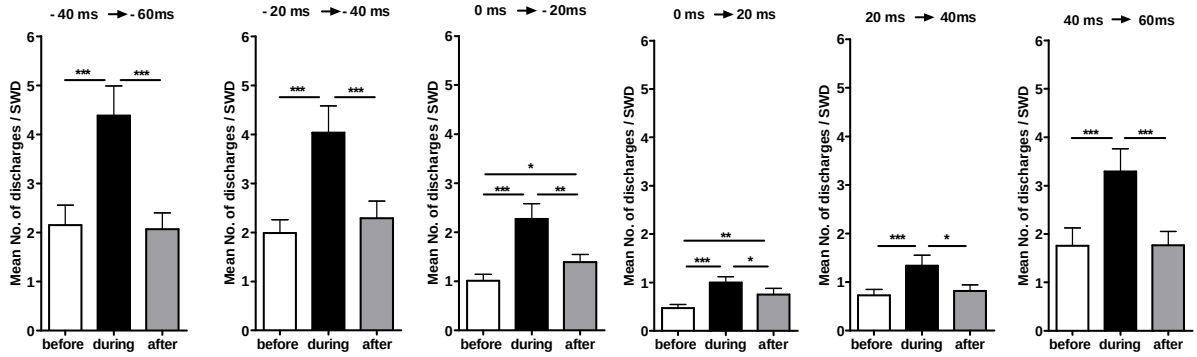

Fig. 3.6: Average number (mean ± SEM) of unit discharges in the PC associated with one SWD on the ECoG. Each diagram shows unit discharges before, during, and after CGP application. At the top of each diagram, the analysed interval with respect to the SWD is given. Negative values indicate intervals before, positive values indicate intervals after the peak component of a SWD. Data obtained from PST histograms, averaged from recordings in 4 neurons. In each neuron, number of cycles was 4. Each cycle contained 75 SWDs.

Significant differences between unit activity before and during CGP application, and between unit activity during and after CGP application, were obtained for all intervals in the early and late phase of SWDs (-40 ms → -60 ms: before vs. during: $p<0.0001$, during vs. after: $p<0.0001$; -20 ms → -40 ms: before vs. during: $p<0.0001$, during vs. after: $p<0.0001$; 0 ms → -20 ms: before vs. during: $p<0.0001$, during vs. after: $p = 0.002$; 0 ms → 20 ms: before vs. during: $p<0.0001$, during vs. after: $p = 0.027$; 20 ms → 40 ms: before vs. during: $p = 0.0005$, during vs. after: $p = 0.027$; 40 ms → 60 ms: before vs. during: $p<0.0001$, during vs. after: $p = 0.0004$). In addition the intervals 0 ms → -20 ms and 0 ms → 20 ms showed significant differences between the unit activity before and after injection of CGP 55845 (0 ms → -20 ms: $p = 0.017$; 0 ms → 20 ms: $p = 0.007$).

In summary, application of CGP 55845 caused an increase in unit activity in the early phase as well as the late phase of SWDs. Unit activity returned to control values during CGP 55845-free periods. While increased activity during bicuculline application was due to prolonged unit activity, increased activity during application of CGP 55845 was due to an increase in action potential frequency. In the presence of CGP, the duration of unit activity remained constant, allowing the conclusion that the inhibitory effect of SWDs on unit activity in PC neurons before and during CGP application was similar. During seizure-free periods there was no significant difference in unit activity before and during CGP 55845 application ($p = 0.3123$, not shown).

3.4 Microstimulation

In a next experimental step, electrical stimuli were locally applied to PC and CL through unilaterally implanted microelectrodes, and the effects on unit activity close to the stimulation site and on ECoG activity were tested. Microstimulation experiments were analysed in 5 (CL) and 8 (PC) WAG/Rij rats.

3.4.1 Microstimulation in the paracentral nucleus

First, main frequencies (5-40 Hz) covering a spectrum of known brain activities (δ-, υ-, β-, and α-oscillations) were tested. As exemplified in figure 3.7, frequencies of 7 Hz and 40 Hz turned out to be the most effective stimulation frequencies. Overall, while stimulation at 7 Hz triggered SWDs following the stimulation frequency, 40 Hz stimulation suppressed SWDs.

3.4.1.1 Stimulation at 7 Hz

During 7 Hz stimulation, bilaterally ECoG-SWDs were present as long as stimulation lasted (7 ± 0.8 s, number of analysed stimulations: n=21). In average, 28 ± 11 s (number of analysed stimulations: n=21) elapsed seizure free until PC neurons were stimulated with 7 Hz. Also 47 ± 15 s (number of analysed stimulations: n=21) after the stimulation, no SWDs occurred. Because the 7 Hz stimulation produced artefacts within the unit recordings (see Fig. 3.7), it is not possible to analyse unit activity in periods of stimulation.

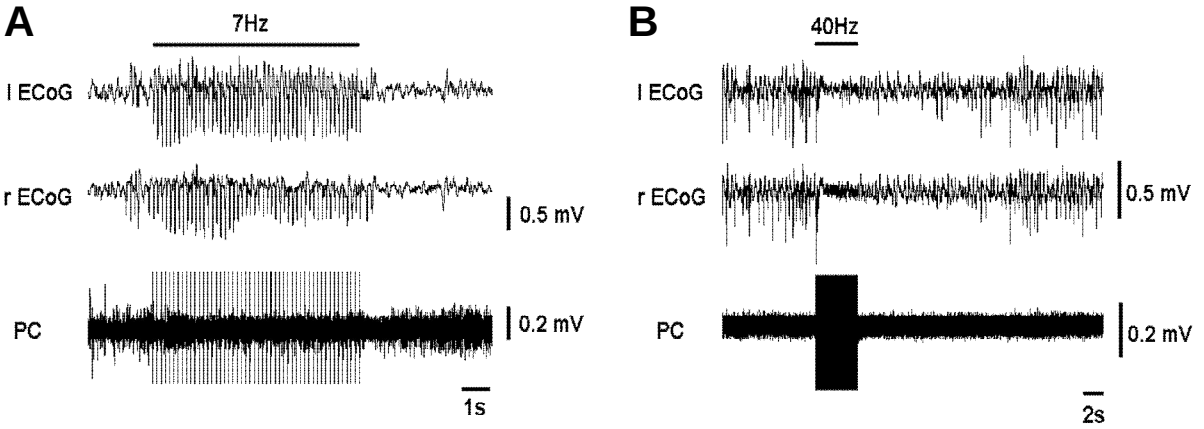

Fig. 3.7: Microstimulation in the PC. Upper and middle traces represent ECoG recordings, lower traces are unit recordings in the PC. **A)** 7 Hz stimulation triggers 7 Hz SWDs in the ECoG. **B)** 40 Hz stimulation interrupts SWDs in the ECoG (see text for details, statistics in Fig. 3.10).

3.4.1.2 Stimulation at 40 Hz

When neurons in the PC were stimulated at 40 Hz, ipsilateral as well as contralateral ECoG-SWDs (with respect to the stimulated hemisphere) were interrupted. Figure 3.10 shows the significant differences between the number of SWDs before and after stimulation (ipsilateral and contralateral: two-tailed paired Student's t test, $p<0.0001$ for all intervals tested).

On average, stimulations lasted 3 ± 0.2 s (number of analysed stimulations: n=54). The recovery of ECoG-SWDs began 21 ± 3 s (number of analysed stimulations: n=54) after the stimulation and usually occurred spontaneously. Surprisingly, not only SWDs disappeared after stimulation with 40 Hz, but also unit activity (Fig. 3.8).

In summary, 7 Hz stimulation triggered SWDs which followed the frequency of stimulation. In contrast, 40 Hz stimulation interrupted SWDs for 21 ± 3 s (number of analysed stimulations: n=54). These effects could be observed on the ipsilateral as well as the contralateral ECoG recording.

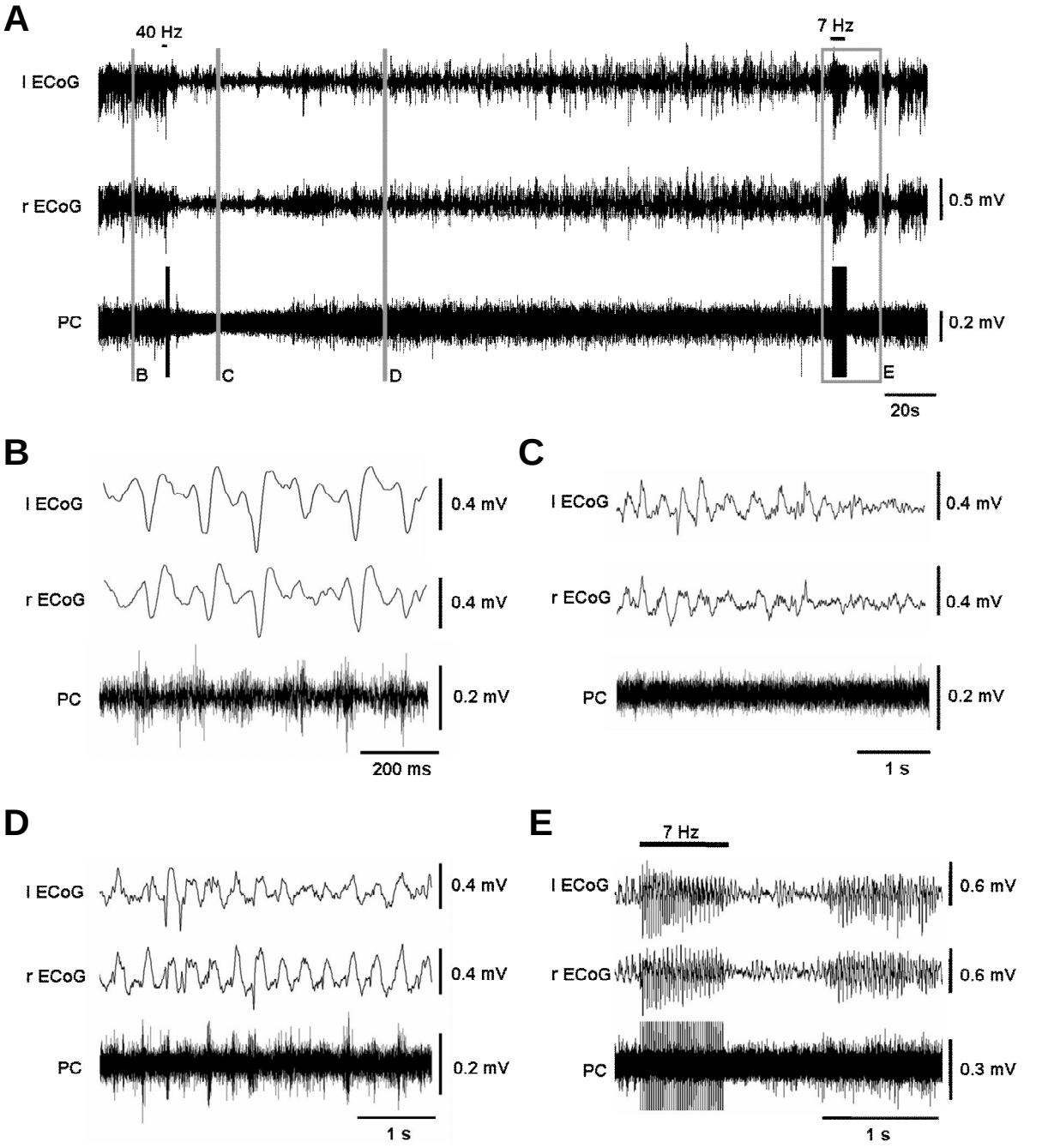

Fig. 3.8: **A)** Example trace of ECoG and unit recordings in the PC. Stimulation (40 Hz and 7 Hz) in the PC was applied during the indicated time periods. Regions marked in grey are shown at an expanded time scale in the devoted figures (B, C, D, E). **B)** Before the stimulation period, SWDs and associated unit activity occurred as described before (Fig. 3.1 B). **C)** Directly after stimulation (40 Hz), SWDs and unit activity were abolished. **D)** Recovery of unit activity began ~45 s after 40 Hz stimulation, during which ECoG recordings showed slow waves with high amplitudes. **E)** 7 Hz stimulation reactivated SWDs, which had been absent before stimulation recommenced. The recovery of SWDs usually occurred spontaneously (see Fig. 3.7B).

3.4.2 Microstimulation in the centrolateral nucleus

Similar microstimulation experiments were performed in the CL. Figure 3.9 shows an example of a typical 7 Hz and 40 Hz stimulation.

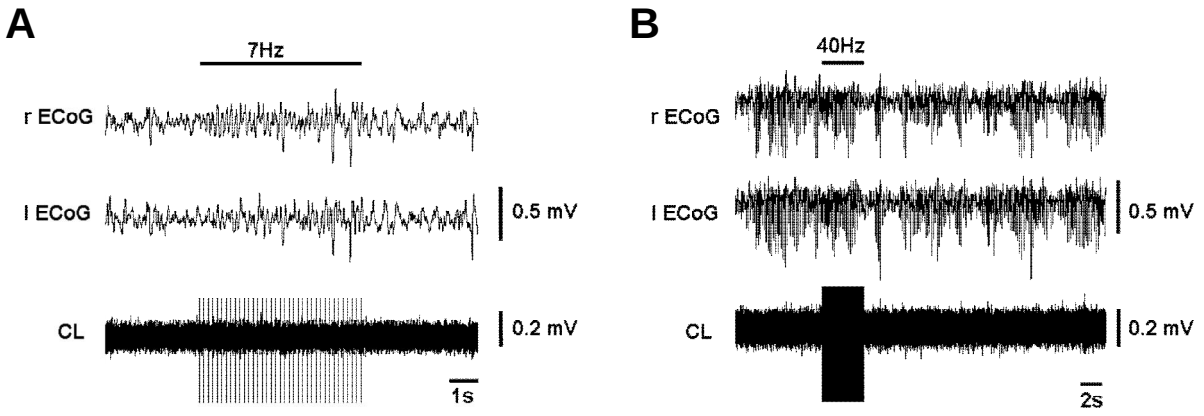

Fig. 3.9: Microstimulation in the centrolateral nucleus (CL). Upper and middle traces represent ECoG recordings, the bottom traces are unit recordings in the CL. **A)** 7 Hz stimulation was not able to trigger 7 Hz SWDs in the ECoG. **B)** 40 Hz stimulation interrupted SWDs in the ECoG to a much lesser degree than in the PC (for details see text, statistics in Fig. 3.10).

3.4.2.1 Stimulation at 7 Hz

In contrast to the PC, 7 Hz stimulation in the CL caused no SWDs in the bilaterally ECoG recordings (Fig. 3.9). On average, 25 ± 7 s (number of analysed stimulations: n=17) elapsed seizure free before the stimulation started. After stimulation, another 65 ± 29 s (number of analysed stimulations: n=17) passed, before SWDs appeared in the ECoG recordings. The duration of stimulation was 7 ± 0.7 s (number of analysed stimulations: n=17).

3.4.2.2 Stimulation at 40 Hz

Stimulation at 40 Hz reduced the number of bilaterally ECoG-SWDs to a much lesser degree than in the PC (Fig. 3.9). However, offline analysis revealed significant differences (ipsilateral: two-tailed paired Student's t: $p<0.0001$ for all analysed intervals; contralateral: *** = $p<0.0001$, * = $p = 0.011$) (see Fig. 3.10).

Although 40 Hz stimulation reduced the number of bilaterally ECoG-SWDs significantly in CL and PC, an obvious long lasting interruption (21 ± 3 s), as observed in the PC, was not observed in the CL (compare Fig. 3.7 B and 3.9 B). After stimulation, the number of SWDs was reduced by about 55% (ipsilateral) and 49% (contralateral) in the PC but only by about 24% (ipsilateral) and 25% (contralateral) in the CL.

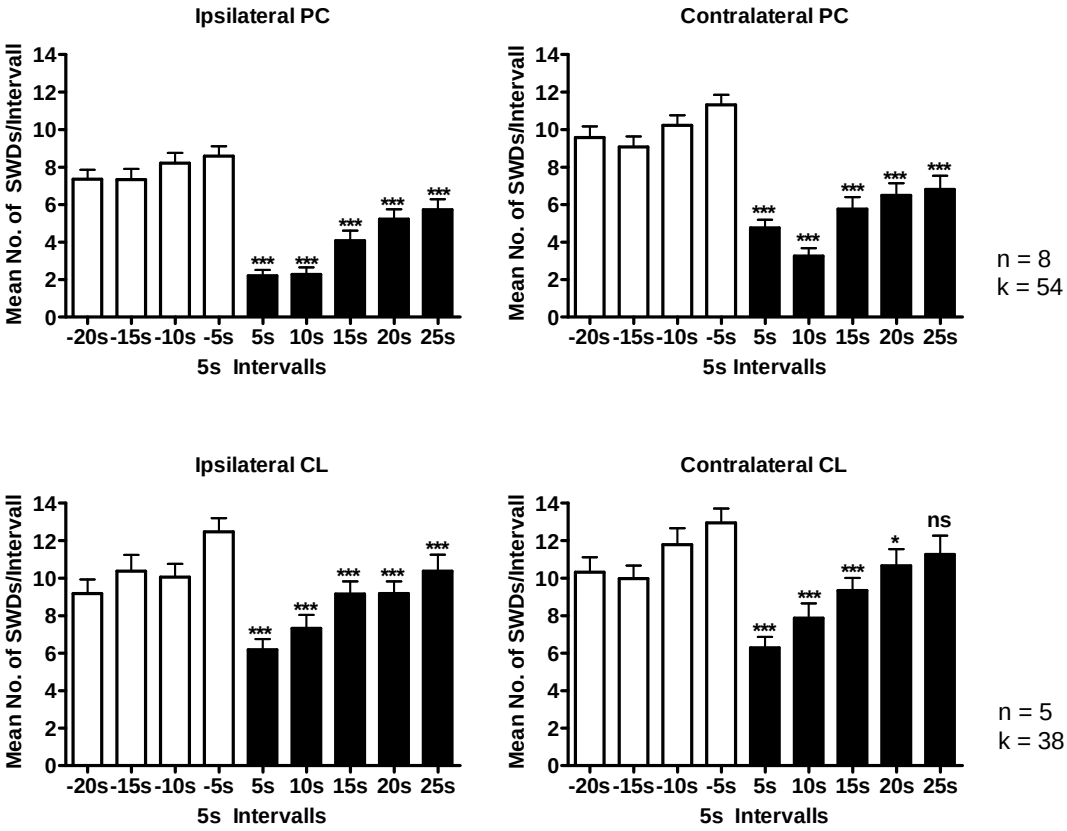

Fig. 3.10: Average number (mean ± SEM) of SWDs in the PC and CL before (white bars) and after (black bars) 40 Hz stimulation. The number of SWDs were analysed in the time period 20 s before and 25 s after the stimulation period. SWDs that occurred within a 5 s window were binned. n, number of animals; k, number of stimulations

In summary, 7 Hz stimulation in the CL did not trigger SWDs, whereas it caused SWDs with exactly that frequency in the PC. Stimulation at 40 Hz reduced the number of SWDs in the CL, but in contrast to stimulation in the PC, no obvious initerruption of seizure activity could be observed on the ECoG.

4. Discussion

The following discussion is divided into three sections, each dealing with specific aspects of the present study. First, the animal model is described with regard to its relevance for absence epilepsy. Second, the historical role of the intralaminar thalamic nuclei for absence epilepsy is highlighted. This section also includes an overview of the anatomical connectivity of intralaminar thalamic nuclei. Third, our findings in the PC are discussed in several subsections. The results of unit recordings in the PC are compared with results obtained from recordings in specific and unspecific thalamic nuclei to highlight the unique role of the PC regarding SWD-related neuronal activity. Next, the role of the intralaminar thalamic nuclei, especially the CL and PC, within the thalamocortical loop is debated. In this context the role of the $GABA_A$ and $GABA_B$ receptors, explored by microiontophoretic applications, are of special interest. Finally, the relevance of the intralaminar thalamic nuclei to SWDs is analysed considering the results of the microstimulation experiments.

4.1 Significance and limitation of WAG/Rij as a genetic model of human absence epilepsy

The validity of the WAG/Rji strain of rats as a model for absence epilepsy in humans can be concluded from: 1) the decrease in responsiveness during the presence of SWDs in both species, 2) the preferential occurrences of SWDs at transitions from states of vigilance to states of light sleep, 3) the suppression and enhancement of SWDs by substances that are effective against human absence seizures and 4) the fact that in both humans and rats absence epilepsy is inherited. Furthermore, sleep deprivation causes the initiation of SWDs in both rats and humans. Two points argue against the eligibility of the WAG/Rij strain of rats as a model for absence epilepsy: 1) in rats absence epilepsy appears after adolescence and persists lifelong, while in humans the seizures occur before adolescence and then either disappear or convert to other forms of epilepsy, 2) the frequency of SWDs is between 5 and 10 Hz in rats and ~3 Hz in humans (Coenen and Van Luijtelaar, 2003). Both points may indicate the involvement of multiple mechanisms and reflect the complexity in the genesis of different forms of SWDs.

The comparison of SWDs in rats and humans is based on unanaesthetised WAG/Rij rats with chronically implanted electrodes. The experiments described here were performed under neurolept anaesthesia. It has been shown that this anaesthesia facilitates the generation of SWDs, without influencing the electrophysiological characteristics of neurons (Inoue et al., 1994). Another rodent model for absence epilepsy is the GAERS strain (Genetic Absence Epilepsy Rats from Strasbourg), which shows the same characteristics (Marescaux and Vergnes, 1995).

4.2 Historical role of the intralaminar thalamic nuclei for absence epilepsy

Early stimulation experiments in cats showed, that SWD-like pattern could be evoked by repetitive stimulation of the unspecific ILTN. This led to the assumption, that the ILTN resemble the centrocephalic pacemaker of absence seizures (Jasper and Droogleever-Fortuyn, 1947). This hypothesis was supported from results which demonstrated, that lesions of the ILTN, but not of the ventroposterior lateral thalamic nucleus, abolished pharmacologically induced SWDs (Banerjee and Snead, 1994). The involvement of the ILTN in the generation of SWDs was supported from unit recordings in rat, which showed that intralaminar thalamic neurons discharge high frequency bursts in correlation with the SWDs (Inoue et al., 1993; Seidenbecher and Pape, 2001). However, these high frequency bursts were delayed with respect to the spike component of the ECoG-SWDs, and thus vote against a pacemaker role of the ILTN. Instead of that, a different scenario for SWD-related activity in ILTN was suggested: the high frequency bursts of ILTN neurons are based on glutamatergic input from the cortex and are additionally controlled through GABAergic influences. Because of the widespread projections of the intralaminar thalamic system tot the cortical system, it was finally suggested that both, GABAergic and glutamatergic influences, may interact during synchronization of neuronal activity, which then converts to rhythmic discharges reflected as SWDs in the ECoG (Seidenbecher and Pape, 2001). To understand these conclusions it is useful to concentrate in a first step on the anatomical connectivity of the ILTN.

4.2.1 Anatomical connection of the intralaminar thalamus

Because our study focused on the CL and PC, the description of the anatomical connectivity of the intralaminar thalamus is restricted to these nuclei here. The CL receives input from the reticular formation, superior colliculus, substantia nigra and the raphe nuclei. Only weak input originates from the periaequaductal grey, locus coeruleus, and some cerebellar nuclei. The PC is targeted by the reticular formation, superior colliculus, supramammillary nucleus and the anterior part of the anterior cingulate cortex (Peschanski and Besson, 1984; Yamasaki et al., 1986; Hallanger et al., 1987; Vertes and Martin, 1988; Vertes, 1991, 1992; Villanueva et al., 1998). The main termination field of the CL in the cerebral cortex is the anterior cingulate cortex that shows fibers in layers I, III and V, in the telencephalon the striatum and in the diencephalon it is the NRT. The PC sends its collaterals to visual cortices and the dorsal anterior cingulate cortex in the cerebral cortex, to the striatum in the telencephalon and to the NRT in the diencephalon (Ullan, 1985; Berendse and Groenewegen, 1991; Groenewegen and Berendse, 1994; Van der Werf et al., 2002).

Although the intralaminar thalamic nuclei receive inputs from various brain areas and project to diverse brain areas, a key role is played by the cortex. Not only that the intralaminar thalamic nuclei target mainly cortical areas in layers I and V (Jones, 1985), but they also receive strong input from the cortex in return, mainly from the cortical layer V (Catsman-Berrevoets and Kuypers, 1978).

Because of this, the intralaminar thalamic nuclei are linked to the thalamocortical loop in two ways: 1) Glutamatergic intralaminar neurons project diffusely to the cortex and receive glutamatergic cortical input on their part (Baughman and Gilbert, 1980; Ottersen et al., 1983; McCormick, 1992). 2) Intralaminar thalamic nuclei get strong GABAergic input from the NRT (Steriade et al., 1984; Kolmac and Mitrofanis, 1997). Because of these interconnections, it was suggested, that the SWD-related burst like discharges in the CL are based on strong glutamatergic input from the cortex and are additionally controlled through GABAergic influences, as mentioned above (Seidenbecher and Pape, 2001).

4.3 Recent results shading new lights onto the role of intralaminar thalamic nuclei

In the present study we used the WAG/Rij strain to investigate the involvement of the intralaminar thalamic nuclei, especially the PC, in the generation of SWDs. The unspecific intralaminar thalamic nuclei are classically assumed to resemble the centrocephalic pacemaker (Jasper and Droogleever-Fortuyn, 1947). Therefore, in our study we aimed to experimentally test the hypothesis that intralaminar thalamic nuclei function as pacemaker of SWDs.

The major findings from the present study are difficult to reconcile with the traditionally proposed role of intralaminar thalamic neurons as pacemakers of SWD, but rather indicate that activity of the PC has to be suppressed to allow SWDs to occur. In detail the findings were: **1)** Neurons of the PC showed tonic activity in seizure-free periods, which was interrupted during the peak component of SWDs. In contrast, unit activity in CL was delayed with respect to the peak component of the SWDs and appeared at random in seizure-free episodes; **2)** Microiontophoretic application of the $GABA_A$ receptor antagonist bicuculline to neurons in the PC caused prolonged activity in the early phase of the SWDs, which resulted in less inhibition during the peak component of the SWDs. When exposed to the $GABA_B$ receptor antagonist CGP neurons displayed an increase in the firing frequency during the late and early phase of SWDs; **3)** Microstimulation experiments in the PC revealed that stimulation with 7 Hz evoked SWDs with exactly that frequency, whereas the same the stimulation parameters in the CL left the ECoG unchanged. Stimulation at 40 Hz in the PC interrupted SWDs for approximately 20 s, whereas stimulation at 40 Hz in the CL only reduced the number of SWDs.

The data obtained from recordings in the CL are a significant extension of previous work (Inoue et al., 1993; Seidenbecher and Pape, 2001). In particular, Inoue and colleagues (1993) found out that discharges in the CL are delayed with respect to the spike component of the SWD in WAG/Rij. This was later confirmed by Seidenbecher and Pape (2001) in GAERS, another genetic rat model of absence epilepsy. Importantly they also observed a tonic firing pattern which preceded the onset of SWDs in one third of the recorded neurons. The present work confirms the delayed firing pattern, whereas the described tonic activity was not detected.

One explanation is that the number of neurons recorded in the CL in the present study was very low (n = 3). The previous study (Seidenbecher and Pape, 2001) also showed that microiontophoretic application of the $GABA_A$ receptor antagonist bicuculline aggravated SWD-related activity in the CL, whereas application of the $GABA_B$ receptor antagonist CGP 35348 had no effect.

Do the findings about neuronal activity in the PC during SWDs, which differs from the activity in the CL, require a new model? Can they be integrated in network functions as previously described? To answer these questions, several aspects of neuronal activity in the PC need to be discussed. First, the results of unit recordings in the PC will be compared with unit recordings from various other thalamic structures. This is required to get an overall idea of neuronal firing patterns and network activity in the thalamus and their contribution to SWDs. Second, the results of the microiontophoresis experiments will be discussed, to speculate about the transmitter systems that may be important in controlling the neuronal activity in the PC. Connectivity will be addressed where required.

4.3.1 Unit recordings demonstrate a delayed recruitment of CL and PC during SWDs

The data presented in this work showed that neurons in the PC fire in a tonic mode in seizure free episodes, whereas tonic activity is inhibited during the peak component of SWDs. This result is not only different to our findings in the CL but also to previous observations (Seidenbecher and Pape, 2001), which showed that unit activity in the PC during SWDs is similar to unit activity in the CL. Thus, regarding the unit recordings, there are three main differences between our results and the previously published work. First, unit activities from our recordings revealed that neurons in the PC are active during the early and late phase of SWDs, whereas the data of the previously mentioned study demonstrate activity only during the late phase of SWDs. Second, the results of the present study showed that neuronal activity in the early and late phase of SWDs is tonic, which is in contrast to the finding of burst like discharges in the late phase of SWDs that was reported previously (Seidenbecher and Pape, 2001). Third, the present study demonstrated tonic activity of PC neurons in seizure free episodes, which is oppositional to the finding that in seizure free episodes neurons in the PC display burst like discharges which appear at random (Seidenbecher and Pape, 2001).
The different findings can be explained by the use of different rat strains.

Here, the WAG/Rij strain was used for studying activity of intralaminar neurons. Seidenbecher and Pape (2001) performed their experiments on the GAERS strain. However there is a study in WAG/Rij rats, which showed a wave-concurrent firing pattern in the PC (Inoue et al., 1993). At first glance this seems to be in accordance to the previously published findings (Seidenbecher and Pape, 2001). But the PST histograms in the study of Inoue et al. (1993) showed not only unit activity in the late but also in the early phase of SWDs, which is in agreement with the findings of the presented work. Another possibility is that neuronal activity in the PC depends on the exact region signals are recorded from, e.g. neurons in the dorsal part of the PC could show different firing patterns than neurons in the ventral part. However, we never observed such differences.

The question, on the impact of PC activity for the generation of SWDs is difficult to answer. To address this question it is feasible to examine SWD-related activity in other, specific and unspecific thalamic nuclei.
Most neurons in specific thalamic nuclei (venteroposteromedial thalamic nucleus (VPM), venteroposterolateral thalamic nucleus (VPL), ventrolateral thalamic nucleus (VL)), show activity which precedes the spike component of the SWD (thus, unit activity is spike correlated). Only neurons in the anteroventral ventrolateral thalamic nucleus (AVVL) display depression of unit activity followed by wave-concurrent excitation (Seidenbecher et al., 1998). In the intralaminar nuclei, unit activity in the centrolateral nucleus is delayed with respect to the peak component of SWDs (thus, unit activity is wave correlated), whereas neurons in the centromedian nucleus show no correlation between unit activity and cortical SWDs (Inoue et al., 1993; Seidenbecher and Pape, 2001). Moreover, neuronal activity in the NRT is associated with spike-concurrent burst like activity (Seidenbecher et al., 1998). Simplified, neuronal activity in specific and unspecific thalamic nuclei seems to be either spike or wave correlated. The results shown in this work are unusual in that they provide evidence for the PC being the only SWD related brain area, that shows spike correlated and wave correlated activity. At best, neurons in the AVVL show activity which is similar to the PC, but to a much lesser degree.

There are some studies which investigated the temporal relationship between thalamic and cortical neuronal activity during SWDs with the aim to reveal network mechanisms responsible for the initiation and generalization of absence seizures (Seidenbecher et al., 1998; Meeren et al., 2002; Polack et al., 2007).

This is usually done by creating a rank order of neuronal activity of different brain regions with respect to the peak component of the SWDs. In that way, the burst firing in the specific thalamic nuclei mentioned above, precedes that in the cortex (Seidenbecher et al., 1998).
This supports the view of a leading role of specific thalamic nuclei during the initiation of SWDs. However, it is now generally accepted that a cortical focus is responsible for the development of SWDs (Meeren et al., 2002; Polack et al., 2007). The contradicting results can be explained by the fact that cortical recordings were obtained from only one recording site in the study of Seidenbecher and Pape (2001). Because cortical unit activity led thalamic unit activity at the start of the SWDs (Seidenbecher et al., 1998), the view of a cortical focus is legitimate.

Keeping the SWD-related activity of neurons of different thalamic nuclei in mind, it is interesting to speculate about the firing pattern of PC neurons. Because of unit activity before and after the peak component of SWDs, it could be assumed that unit activity during the late phase of SWDs is controlled by the cortex (as suggested for the CL, Seidenbecher and Pape, 2001), whereas unit activity during the early phase of SWDs is controlled by a subcortical structure. Thus, two independent inputs could control activity in the PC and lead to two burst like discharges – one in the early phase and one in the late phase of SWDs. Indeed, the calculated PST histograms of unit recordings indicate that neuronal activity is reduced for a relatively short time period before the peak component of SWDs and that the reactivation of neuronal activity takes more time. Therefore, it is more likely that unit activity in the PC reflects tonic discharges which are interrupted during the peak component of SWDs. In favour of that, PC neurons also show tonic activity during seizure-free episodes and do not display burst like discharges. Taken together, these findings support the notion that neuronal activity in the PC has to be suppressed to allow SWDs to be initiated.
But what is the underlying mechanism of this suppression? To answer this question, the results of microiontophoresis experiments performed in the course of this study need to be discussed.

4.3.2 Microiontophoretic experiments indicate a role of GABAergic inhibition

The results showed that microiontophoretic application of the $GABA_A$ receptor antagonist bicuculline and the $GABA_B$ receptor antagonist CGP result both in increasing neuronal activity in the PC. This indicates that GABAergic processes, which inhibit neuronal activity during SWDs, are active in the PC. The main GABAergic input to the PC comes from the NRT (Steriade et al., 1984; Kolmac and Mitrofanis, 1997), and therefore, its integration to the thalamocortical loop and its role in the generation of diverse brain rhythms should be kept in mind. NRT neurons, which receive input from the cortex, produce burst discharges which result in a release of GABA onto thalamocortical neurons in thalamic relay nuclei. As a result, thalamocortical neurons produce rebound burst discharges, which are transferred back to neurons in the NRT via glutamatergic axon collaterals. This causes burst discharges in the NRT, and the cycle starts again (Steriade et al., 1993b; von Krosigk et al., 1993; Bal et al., 1995; McCormick and Bal, 1997). Thus, cyclical interaction between thalamocortical and NRT neurons generate spindle waves, which are observable in the EEG (Contreras and Steriade, 1995).

It is generally accepted that the development of SWDs is associated with an increase in synchronization in the thalamocortical network (Steriade et al., 1994). Although the structural and physiological basis underlying the pathological transformation of these rhythms into SWDs seems to be GABAergic, the degree of contribution of $GABA_A$ and $GABA_B$ receptors to these transformations is not yet fully understood. For instance, early studies showed that $GABA_B$ receptors are crucial for 'preparing' thalamocortical cells for burst firing by activating LTS (Crunelli and Leresche, 1991). In line with this finding is that in chronically implanted GAERS, thalamic injections of a $GABA_B$ receptor agonist increased the incidence of SWDs, whereas it was decreased by injections of a $GABA_B$ receptor antagonist (Liu et al., 1992). An *in vitro* study suggested that the described $GABA_B$ effects were based on the fact that activation of $GABA_B$ receptors caused a stronger activation of the LTS, which will result in larger-than-usual rebound bursts (von Krosigk et al., 1993).

Further *in vitro* studies found out that increased input from relay cells to the cortex or the NRT can enhance $GABA_B$ responses and, therefore, facilitate transformation from spindle waves to SWDs (Kim et al., 1997; Bal et al., 2000; Blumenfeld and McCormick, 2000). However, intracellular recordings in GAERS demonstrated that IPSPs, which are active during SWDs, are mediated by activation of $GABA_A$ but not $GABA_B$ receptors (Pinault et al., 1998; Charpier et al., 1999).

A contribution of $GABA_B$ receptors was not excluded: it was suggested that the tonic hyperpolarization of thalamocortical relay cells during SWDs is due to long lasting $GABA_B$ IPSPs (Charpier et al., 1999). Nevertheless, microiontophoresis studies showed that application of a $GABA_B$ receptor antagonist to neurons of specific thalamic nuclei had no effect to neuronal activity, which argues against a significant role of this receptor to the generation of SWDs (Staak and Pape, 2001). Interestingly, when Staak and Pape (2001) pharmacologically blocked the $GABA_A$ receptors, they observed that $GABA_B$ receptors are also active. They suggested that the reason for this is an increase in $GABA_B$ mediated IPSPs in consequence of a blockade of $GABA_A$ receptors, and that the underlying mechanism is a reduction in the shunting effect of the $GABA_A$ chloride conductance. In addition, whole cell patch clamp recordings in the somatosensory cortex, ventrobasal thalamus (VB), and NRT indicated that SWDs are related to alterations of $GABA_A$ mediated inhibition in the NRT, without an involvement of $GABA_B$ receptors (Bessaih et al., 2006).

Taken together, it seems likely that both $GABA_A$ and $GABA_B$ receptors participate in the generation of SWDs. In particular $GABA_A$ receptor are involved in high frequent SWDs (7-11 Hz), whereas $GABA_B$ receptors play a role in the generation of low frequent SWD (3 Hz), Indeed, it is conspicuous that most studies which highlighted the role of the $GABA_B$ receptor are *in vitro* studies, whereas most *in vivo* studies support the $GABA_A$ receptor. Two reasons argue for $GABA_A$ receptors to be more prominent: 1) in *in vivo* studies, results are obtained within an intact neuronal network, which more closely resembles the physiological properties in a living organism; 2) the involvement of $GABA_B$ receptors in seizure-activity became visible after blockade of $GABA_A$ receptors. However, it is possible that anaesthesia in *in vivo* studies alters the properties of different receptors by its action on ion channels and receptors in synapses. In the present study, Fentanyl and Droperidol were used for a neurolept anaesthesia. Both drugs interact with GABA receptors: Droperidol inhibits the activation of $GABA_A$ receptors, Fentanyl diminishes the overall GABA release (Flood and Coates, 2002; Kouvaras et al., 2008). Thus, the results of the microiontophoresis experiments do not necessarily reflect the physiological state. Nevertheless, this is unlikely to play a role in the results obtained here, because no quantification of GABAergic mechanisms were made. The present study rather investigates whether GABA receptors are active during SWDs or not and thus, whether they are important in the generation of SWDs. Because both $GABA_A$ and $GABA_B$ receptors are found to participate in neuronal activity of PC neurons during SWDs, the described effects of Fentanyl and Droperidol can be considered to be negligible.

In summary, GABA induced rebound bursts in thalamocortical relay cells seem to be important for SWD-related activity in specific thalamic nuclei.

In intralaminar thalamic nuclei, a different scenario for SWD-related activity was suggested (Seidenbecher and Pape, 2001): glutamatergic input from the cortex causes burst activity in the PC and CL, which is controlled through GABAergic input from the NRT (see above).
Their data also indicated that the GABAergic input acts on $GABA_A$ but not on $GABA_B$ receptors. This is in contrast to the findings presented in this work which indicates that $GABA_A$ as well as $GABA_B$ receptors are active during SWDs. The contradicting results may be explained by the use of different $GABA_B$ receptor blockers. Here, an antagonist was chosen (CGP 55845) that is approximately 10000fold more potent than the antagonist used in the above-mentioned study (CGP 35348). Apart from the different findings regarding $GABA_B$ receptors, the suggested model seems to be sufficient to explain the firing pattern we observed in the PC: neurons in the PC receive glutamatergic input and are thus tonically active. GABAergic input from the NRT acts on $GABA_A$ and $GABA_B$ receptors in PC neurons and, thus, inhibits tonic activity during the peak component of the SWDs. To answer the question asked at the beginning of this discussion: the observed firing pattern of neurons in the PC may be explained by the same model as suggested previously (Seidenbecher and Pape, 2001). However, the results of the present work indicated that glutamatergic input produces burst firing in the CL and tonic activity in the PC, whereas the previously mentioned study suggested that the cortical input causes burst firing in both, the PC and CL. This behaviour may be explained by two separate scenarios: either neurons in both nuclei have different intrinsic properties or they receive input from different brain structures. Certainly, a combination of both possibilities seems plausible.
Recordings *in vivo* and *in vitro* showed that CL neurons express prominent I_T and are able to generate LTS bursts (Domich et al., 1986; Lacey et al., 2007, Broicher et al., 2008). Thus, CL neurons have properties that are typical of thalamic relay neurons. The intrinsic properties of PC neurons remain largely unknown. It was suggested that all thalamocortical relay cells have the same fundamental properties (Llinas and Steriade, 2006).

Regarding this, data from in vivo and in vitro studies allow the suggestion that neurons in the Pf have unusual intrinsic properties in that they show only little, if any, LTS (Phelan et al., 2005; Smith et al., 2006; Lacey et al., 2007). Thus, it is possible that PC neurons have distinct intrinsic properties in comparison to the 'normal' thalamocortical relay cells. An easy explanation for the different firing behaviour in CL and PC neurons could be that neurons in the CL are in a hyperpolarized state, whereas PC neurons are depolarized.
The anatomical connectivity of the CL and PC seems not to be different. Therefore, it does not seem feasible to make different connectivity accountable for the different results we observed in the CL and PC. Nevertheless, the superior colliculus (SC), which projects to the intralaminar thalamic nuclei, could provide an explanation for our findings, because electrical and pharmacological studies showed that activation of the superior colliculus suppresses absence seizures (Nail-Boucherie et al., 2002; Nail-Boucherie et al., 2005). It was assumed, that activation of the SC may enhance the release of glutamate onto neurons of the PF, which would result in an increase of activity of PF neurons and, thereby, could lead to seizure suppression. In other words, activity in the PF has to be suppressed to allow occurrence of SWDs, which is what has been stated for the PC here. Although the microiontophoretic experiments indicated that increased activity of PC neurons results in less inhibition during the peak component of the SWDs, no change in the incidence of SWDs was observed in the ECoG. Because microiontophoretic application can only alter the activity of neurons directly adjacent to the electrode tip, this method does not allow to change the activity of a whole network. Thus, it is not surprising that no alterations of the SWDs were noticeable in the ECoG. A method to stimulate a large number of neurons and, thus, change network activity in such a way that also the ECoG recordings are influenced, is microstimulation.

In summary, it seems feasible, that GABAergic processes, which suppress neuronal activity during SWDs, are active in the PC. Because application of both, $GABA_A$ receptor antagonist bicuculline and $GABA_B$ receptor antagonist CGP, result in increasing neuronal activity in the PC, there is evidence, that GABAergic input act on $GABA_A$ and $GABA_B$ receptors in PC neurons and, thus, inhibits tonic activity during the peak component of the SWDs.

4.3.3 Microstimulation experiments suggest a frequency-dependent recruitment

In humans, deep brain stimulation is currently discussed as an effective treatment for epilepsy. Target regions for antiepileptic deep brain stimulation are the cerebellum, the subthalamic nucleus, the caudate nucleus and the thalamus (Schulze-Bonhage, 2009). In the thalamus, one effective region for stimulation was found to be the CM (Fisher et al., 1992; Velasco et al., 2001; Velasco et al., 2006). However, the effects of microstimulation in the ILTN of rats remain largely unknown.

In the present study it was observed that stimulation of the PC at 40 Hz interrupted SWDs, whereas it was ineffective in the CL. In the PC, stimulation at 7 Hz triggered 7 Hz SWDs, whereas no effect was visible in the ECoG when stimulating the CL. This might indicate that the anatomical network of both structures operates quite differently, although their connectivity seems to be nearly identical (Ullan, 1985; Berendse and Groenewegen, 1991; Groenewegen and Berendse, 1994; Van der Werf et al., 2002). For instance, the transmitter release onto cortical neurons could be less effective in the CL than in the PC. Further analyses are needed to clarify this.

Unit recordings showed that tonic activity in the PC is inhibited during the peak component of SWDs. Thus it was expected, that activity of the PC neurons has to be enhanced to achieve a disinhibition during the peak component of the SWDs, which in turn should result in a suppression of SWDs. Surprisingly, neurons in the PC are inactive during interruption of SWDs. Because during microstimulation both somata and fibres are stimulated, one possible explanation could be, that voltage gated ion channels in the somatic plasma membrane are activated. This could cause an inhibition of PC neurons, whereas nevertheless Na^+/K^+ action potentials would be generated in the fibres. These could in turn increase the transmitter release onto cortical neurons. For instance, the KCNQ-type potassium channels, generating the inhibitory M-type current, come into consideration as inhibitory voltage gated channels. Immunohistochemical experiments in the mouse brain showed that this channel is expressed in the thalamus (Geiger et al., 2006). It has been shown that GABAergic neurons are distributed in the intralaminar thalamic nuclei (Hunt et al., 1991). Thus, it is also possible that stimulation of intralaminar neurons activates GABAergic neurons, which project back to the ILTN, and thereby cause an inhibition of intralaminar neurons. Furthermore, because of the relatively large diameter of the stimulation electrode in relation to the diameter of the PC, it is not unlikely, that the stimulation electrode not only acts on the PC but also on fibres which project to this nucleus.

In that manner, stimulated GABAergig fibres of the NRT, substantia nigra, and zona incerta could exert an inhibitory influence onto the PC neurons (Huguenard and McCormick, 2007).

Finally, the question, why different stimulation frequencies produce different ECoG patterns has to be answered. There is evidence from two studies which combined in vitro thalamic slice models with an artificial cortical network, that cortical feedback, which was triggered by spindle activity, could transform thalamic oscillations into slow, synchronous oscillations (Bal et al., 2000; Blumenfeld and McCormick, 2000). Based on these results, it was suggested that a modest increase in cortical excitability, when it is in a range that produces constructive interference with the network, causes a transformation of spindle waves to SWDs. On the opposite, excitatory feedback, which produces destructive interferences, destabilizes the development of global oscillations (Huguenard and McCormick, 2007). The results of the present study are in accordance to this model: 7 Hz stimulation was able to produce constructive interference and, therefore, generated SWDs, whereas 40 Hz stimulation provoked destructive interference and, thereby, suppressed the occurrence of SWDs.

In summary, stimulation of the CL at 40 Hz and 7 Hz was ineffective. In contrast, stimulation of the PC at 40 Hz interrupted SWDs, whereas stimulation at 7 Hz triggered 7 Hz SWDs. These findings indicate that both nuclei have a different function, although their anatomical connectivity seems to be nearly identical.

4.4 Concluding remarks and outlook

The main purpose of the present study was to investigate the ILTN with respect to their potential role as pacemakers of SWDs, with particular reference to PC. In general, our findings do not support the proposed role of PC neurons to function as pacemakers of SWDs. On the contrary, activity of PC neurons had to be suppressed to allow the occurrence of SWDs. It is important to note that this is a unique feature of the PC. SWD-related activities in the other ILTN not only differ from those in the PC, but also each have their own characteristic firing behaviour: the CL displays burst correlated activity, the Pf shows spike correlated activity, and neuronal activity in the CM is not correlated to SWDs at all (personal observation and Inoue et al., 1993; Seidenbecher and Pape, 2001).

Thus, it seems likely that the nuclei of the intralaminar thalamus have functional differences, which is remarkable in that most studies on ILTN tend to transfer obtained results from a specific intralaminar thalamic nuclei to the whole intralaminar thalamus (for instance, Groenewegen and Berendse, 1994). The concept of functional differences of the ILTN is also supported by the results obtained from our microstimulation experiments in the CL and PC: microstimulation of PC neurons depressed or recruited SWDs on the ECoG, depending on the used stimulation-frequency, whereas stimulation of CL neurons had no effect.
Thus, the question which contribution the ILTN make to the generation of SWDs has to be answered individually for all nuclei of the intralaminar thalamus. The present study highlighted the importance of PC neurons in absence epilepsy by showing their influence on SWDs on a network level, and by demonstrating their dependency on GABAergic mechanisms during SWDs on a molecular level. However, further studies are needed to investigate the contribution of the other ILTN to absence epilepsy, and to explore their interactions among themselves. Moreover, the assumption, that the intralaminar thalamic network interacts with the cortical system (through glutamateric input from the cortex and GABEergic input from the NRT) during synchronization of cellular activities towards generation of rhythmic discharges, has to be proved in future studies.

At present, about a third of patients with epilepsy continue to be subject to seizures even after attempted treatment with a wide variety of antiepileptic drugs (Schulze-Bonhabe, 2009). Thus, the study of elementary neuronal mechanisms of epilepsy is crucial to develop new strategies in the treatment of epilepsy. Especially the exploration of epilepsy on the molecular level (i.e. microiontophoretic experiments) can give important hints to evolve new, more efficient antiepileptic drugs. For some forms of epilepsy, also surgery can achieve freedom from seizures. Because in some cases no circumscribed focus can be identified or because its removal would entail risking the impairment of cognitive or motor function, not all patients can benefit from a surgery. This is why it is particularly important to develop alternative therapeutic techniques. Up to date, deep brain stimulation is discussed as a new possibility for an innovative treatment for epilepsy (Schulze-Bonhabe, 2009). In this context, microstimulation experiments in animal are needed to get detailed knowledge about effective stimulation parameters and loci.

5. References

Avoli M, Rogawski AM, Avanzini G (2001) Generalized Epileptic Disorders: An Update. Epilepsia 42:445-457.

Bal T, von Krosigk M, McCormick DA (1995) Role of the ferret perigeniculate nucleus in the generation of synchronized oscillations in vitro. J Physiol 483 (Pt 3):665-685.

Bal T, Debay D, Destexhe A (2000) Cortical Feedback Controls the Frequency and Synchrony of Oscillations in the Visual Thalamus. J Neurosci 20:7478-7488.

Banarjee PK, Snead OC (1994) Thalamic mediodorsal and intralaminar nuclear lesions disrupt the generation of experimentally induced generalized absence-like seizures in rats. Epilepsy Res 17:193-205.

Baughman RW, Gilbert CD (1980) Aspartate and glutamate as possible neurotransmitters of cells in layer 6 of the visual cortex. Nature 287:848-850.

Berendse HW, Groenewegen HJ (1991) Restricted cortical termination fields of the midline and intralaminar thalamic nuclei in the rat. Neuroscience 42:73-102.

Bessaih T, Bourgeais L, Badiu CI, Carter DA, Toth TI, Ruano D, Lambolez B, Crunelli V, Leresche N (2006) Nucleus-specific abnormalities of GABAergic synaptic transmission in a genetic model of absence seizures. J Neurophysiol 96:3074-3081.

Blom S, Heubel J, Bergfors PG (1972) Benign Epilepsy of Children with Centro-temporal EEG Foci. Prevalence and follow-up study of 40 patients. Epilepsia 13:609.

Blumenfeld H, McCormick DA (2000) Corticothalamic inputs control the pattern of activity generated in thalamocortical networks. J Neurosci 20:5153-5162.

Broicher T, Kanyshkova T, Meuth P, Pape HC, Budde T (2008) Correlation of T-channel coding gene expression, I_T, and the low threshold Ca^{2+} spike in the thalamus of a rat model of absence epilepsy. Mol Cell Neurosci. 39(3):384-399.

Budde T, Caputi L, Kanyshkova T, Staak R, Abrahamczik C, Munsch T, Pape HC (2005a) Impaired regulation of thalamic pacemaker channels through an imbalance of subunit expression in absence epilepsy. J Neurosci 25:9871-9882.

Catsman-Berrevoets CE, Kuypers HG (1978) Differential laminar distribution of corticothalamic neurons projecting to the VL and the center median. An HRP study in the cynomolgus monkey. Brain Res 154:359-365.

Charpier S, Leresche N, Deniau JM, Mahon S, Hughes SW, Crunelli V (1999) On the putative contribution of GABA(B) receptors to the electrical events occurring during spontaneous spike and wave discharges. Neuropharmacol 38:1699-1706.

Coenen AM, Van Luijtelaar EL (2003) Genetic animal models for absence epilepsy: a review of the WAG/Rij strain of rats. Behav Genet 33:635-655.

Contreras D, Steriade M (1995) Cellular basis of EEG slow rhythms: a study of dynamic corticothalamic relationships. J Neurosci 15:604-622.

Crunelli V, Leresche N (1991) A role for GABAB receptors in excitation and inhibition of thalamocortical cells. Trends Neurosci 14:16-21.

Crunelli V, Leresche N (2002) Childhood absence epilepsy: genes, channels, neurons and networks. Nat Rev Neurosci 3:371-382.

Domich L, Oakson G, Steriade M (1986) Thalamic burst patterns in the naturally sleeping cat: a comparison between cortically projecting and reticularis neurones. J Physiol 379:429-449.

Fisher RS, Uematsu S, Krauss GL, Cysyk BJ, McPherson R, Lesser RP, Gordon B, Schwerdt P, Rise M (1992) Placebo-controlled pilot study of centromedian thalamic stimulation in treatment of intractable seizures. Epilepsia 33:841-851.

Flood P, Coates KM (2002) Droperidol Inhibits GABAA and Neuronal Nicotinic Receptor Activation. Anesthesiol 96:987-993.

Geiger J, Weber YG, Landwehrmeyer B, Sommer C, Lerche H (2006) Immunohistochemical analysis of KCNQ3 potassium channels in mouse brain. Neurosci Lett 400:101-104.

Gloor P (1968) Generalized Cortico-Reticular Epilepsies Some Considerations on the Pathophysiology of Generalized Bilaterally Synchronous Spike and Wave Discharge. Epilepsia 9:249-263.

Groenewegen HJ, Berendse HW (1994) The specificity of the 'nonspecific' midline and intralaminar thalamic nuclei. Trends Neurosci 17:52-57.

Hallanger AE, Levey AI, Lee HJ, Rye DB, Wainer BH (1987) The origins of cholinergic and other subcortical afferents to the thalamus in the rat. J Comp Neurol 262:105-124.

Hobson JA, Pace-Schott EF (2002) The cognitive neuroscience of sleep: neuronal systems, consciousness and learning. Nat Rev Neurosci 3:679-693.

Huguenard JR, McCormick DA (2007) Thalamic synchrony and dynamic regulation of global forebrain oscillations. Trends Neurosci 30:350-356.

Hunt CA, Pang DZ, Jones EG (1991) Distribution and density of GABA cells in intralaminar and adjacent nuclei of monkey thalamus. Neuroscience 43:185-196.

Inoue M, Duysens J, Vossen JM, Coenen AM (1993) Thalamic multiple-unit activity underlying spike-wave discharges in anesthetized rats. Brain Res 612:35-40.

Inoue M, Ates N, Vossen JMH, Coenen AML (1994) Effects of the neuroleptanalgesic fentanyl-fluanisone (Hypnorm) on spike-wave discharges in epileptic rats. Pharmacol Biochem and Behav 48:547-551.

Jahnsen H, Llinas R (1984a) Ionic basis for the electro-responsiveness and oscillatory properties of guinea-pig thalamic neurones in vitro. J Physiol 349:227-247.

Jahnsen H, Llinas R (1984b) Electrophysiological properties of guinea-pig thalamic neurones: an in vitro study. J Physiol 349:205-226.

Jahnsen H, Llinas R (1984c) Voltage-dependent burst-to-tonic switching of thalamic cell activity: an in vitro study. Arch Ital Biol 122:73-82.

Jasper HH, Droogleever-Fortuyn J (1947) Experimental Studies on the Functional Anatomy of Petit Mal Epilepsy. Res Publ Ass Res Nerv Ment Dis 26:272-298.

Jones EG (1985) The Thalamus. Plenum Press, New York.

Kim U, Sanchez-Vives MV, McCormick DA (1997) Functional dynamics of GABAergic inhibition in the thalamus. Science 278:130-134.

Kolmac CI, Mitrofanis J (1997) Organisation of the reticular thalamic projection to the intralaminar and midline nuclei in rats. J Comp Neurol 377:165-178.

Kouvaras E, Asprodini EK, Asouchidou I, Vasilaki A, Kilindris T, Michaloudis D, Koukoutianou I, Papatheodoropoulos C, Kostopoulos G (2008) Fentanyl treatment reduces GABAergic inhibition in the CA1 area of the hippocampus 24 h after acute exposure to the drug. Neuropharmacol 55:1172-1182.

Lacey CJ, Bolam JP, Magill PJ (2007) Novel and distinct operational principles of intralaminar thalamic neurons and their striatal projections. J Neurosci 27:4374-4384.

Liu Z, Vergnes M, Depaulis A, Marescaux C (1992) Involvement of intrathalamic GABAB neurotransmission in the control of absence seizures in the rat. Neuroscience 48:87-93.

Llinas RR, Steriade M (2006) Bursting of Thalamic Neurons and States of Vigilance. J Neurophysiol 95:3297-3308.

Lopez J, Wolff M, Lecourtier L, Cosquer B, Bontempi B, Dalrymple-Alford J, Cassel J-C (2009) The Intralaminar Thalamic Nuclei Contribute to Remote Spatial Memory. J Neurosci 29:3302-3306.

Marescaux C, Vergnes M (1995) Genetic Absence Epilepsy in Rats from Strasbourg (GAERS). Ital J Neurol Sci 16:113-118.

McCormick DA (1992) Neurotransmitter actions in the thalamus and cerebral cortex and their role in neuromodulation of thalamocortical activity. Prog Neurobiol 39:337-388.

McCormick DA, Pape HC (1990) Properties of a hyperpolarization-activated cation current and its role in rhythmic oscillation in thalamic relay neurones. J Physiol 431:291-318.

McCormick DA, Bal T (1997) Sleep and arousal: thalamocortical mechanisms. Annu Rev Neurosci 20:185-215.

Meeren HK, Pijn JP, Van Luijtelaar EL, Coenen AM, Lopes da Silva FH (2002) Cortical focus drives widespread corticothalamic networks during spontaneous absence seizures in rats. J Neurosci 22:1480-1495.

Nail-Boucherie K, Lê-Pham BT, Marescaux C, Depaulis A (2002) Suppression of Absence Seizures by Electrical and Pharmacological Activation of the Caudal Superior Colliculus in a Genetic Model of Absence Epilepsy in the Rat. Exp Neurol 177:503-514.

Nail-Boucherie K, Le-Pham BT, Gobaille S, Maitre M, Aunis D, Depaulis A (2005) Evidence for a role of the parafascicular nucleus of the thalamus in the control of epileptic seizures by the superior colliculus. Epilepsia 46:141-145.

Ottersen OP, Fischer BO, Storm-Mathisen J (1983) Retrograde transport of D-[3H]aspartate in thalamocortical neurones. Neurosci Lett 42:19-24.

Pace-Schott EF, Hobson JA (2002) The neurobiology of sleep: genetics, cellular physiology and subcortical networks. Nat Rev Neurosci 3:591-605.

Panayiotopoulos PC (2008) Typical absence seizures and related epileptic syndromes: Assessment of current state and directions for future research. Epilepsia 49:2131-2139.

Pape HC, Meuth SG, Seidenbecher T, Munsch T, Budde T (2005) Der Thalamus: Tor zum Bewusstsein und Rhytmusgenerator im Gehirn. Neuroforum 02:44-54.

Paxinos G, Watson C (1998) The Rat Brain in Stereotaxic Coordinates. 4th edn. Academic Press, New York.

Peschanski M, Besson JM (1984) A spino-reticulo-thalamic pathway in the rat: An anatomical study with reference to pain transmission. Neuroscience 12:165-178.

Phelan KD, Mahler HR, Deere T, Cross CB, Good C, Garcia-Rill E (2005) Postnatal maturational properties of rat parafascicular thalamic neurons recorded in vitro. Thalamus Relat Syst 3:89-113.

Pinault D, Leresche N, Charpier S, Deniau JM, Marescaux C, Vergnes M, Crunelli V (1998) Intracellular recordings in thalamic neurones during spontaneous spike and wave discharges in rats with absence epilepsy. J Physiol 509 (Pt 2):449-456.

Polack PO, Guillemain I, Hu E, Deransart C, Depaulis A, Charpier S (2007) Deep layer somatosensory cortical neurons initiate spike-and-wave discharges in a genetic model of absence seizures. J Neurosci 27:6590-6599.

Ren Y, Zhang L, Lu Y, Yang H, Westlund KN (2009) Central Lateral Thalamic Neurons Receive Noxious Visceral Mechanical and Chemical Input in Rats. J Physiol 102:244-258.

Schulze-Bonhage A (2009) Deep brain stimulation: a new approach to the treatment of epilepsy. Dtsch Arztebl Int 106:407-412.

Seidenbecher T, Pape HC (2001) Contribution of intralaminar thalamic nuclei to spike-and-wave-discharges during spontaneous seizures in a genetic rat model of absence epilepsy. Eur J Neurosci 13:1537-1546.

Seidenbecher T, Staak R, Pape HC (1998) Relations between cortical and thalamic cellular activities during absence seizures in rats. Eur J Neurosci 10:1103-1112.

Sherman SM, Guillery RW (2006) Exploring the Thalamus and Its Role in Cortical Function. Cambridge, Massachusetts: MIT Press.

Smith PH, Bartlett EL, Kowalkowski A (2006) Unique combination of anatomy and physiology in cells of the rat paralaminar thalamic nuclei adjacent to the medial geniculate body. J Comp Neurol 496:314-334.

Staak R, Pape HC (2001) Contribution of GABA(A) and GABA(B) receptors to thalamic neuronal activity during spontaneous absence seizures in rats. J Neurosci 21:1378-1384.

Steriade M (2005) Sleep, epilepsy and thalamic reticular inhibitory neurons. Trends Neurosci 28:317-324.

Steriade M, Deschenes M (1984) The thalamus as a neuronal oscillator. Brain Res 8:1-63.

Steriade M, Llinas RR (1988) The functional states of the thalamus and the associated neuronal interplay. Physiol Rev 68:649-742.

Steriade M, Timofeev I (2003) Neuronal plasticity in thalamocortical networks during sleep and waking oscillations. Neuron 37:563-576.

Steriade M, Amzica F (2003) Sleep oscillations developing into seizures in corticothalamic systems. Epilepsia 44 Suppl 12:9-20.

Steriade M, Parent A, Hada J (1984) Thalamic projections of nucleus reticularis thalami of cat: a study using retrograde transport of horseradish peroxidase and fluorescent tracers. J Comp Neurol 229:531-547.

Steriade M, Dossi RC, Contreras D (1993a) Electrophysiological properties of intralaminar thalamocortical cells discharging rhythmic (~40 HZ) spike-bursts at ~1000 HZ during waking and rapid eye movement sleep. Neuroscience 56:1-9.

Steriade M, McCormick DA, Sejnowski TJ (1993b) Thalamocortical oscillations in the sleeping and aroused brain. Science 262:679-685.

Steriade M, Contreras D, Amzica F (1994) Synchronized sleep oscillations and their paroxysmal developments. Trends Neurosci 17:199-208.

Talley EM, Solorzano G, Depaulis A, Perez-Reyes E. Bayliss DA (2000) Low-voltage-activated calcium channel subunit expression in a genetic model of absence epilepsy in the rat. Brain Res Mol Brain Res 75:159-165.

Tsakiridou E, Bertollini L, De Curtis M, Avanzini G, Pape HC (1995) Selective increase in T-Type calcium conductance of reticular thalamic neurons in a rat model of absence epilepsy. J Neurosci 15:3110-3117

Ullan J (1985) Cortical topography of thalamic intralaminar nuclei. Brain Res 328:333-340.

Van der Werf YD, Witter MP, Groenewegen HJ (2002) The intralaminar and midline nuclei of the thalamus. Anatomical and functional evidence for participation in processes of arousal and awareness. Brain Res Brain Res Rev 39:107-140.

Van Luijtelaar EL, Drinkenburg WH, Van Rijn CM, Coenen AM (2002) Rat models of genetic absence epilepsy: what do EEG spike-wave discharges tell us about drug effects? Methods Find Exp Clin Pharmacol 24 Suppl D:65-70.

Velasco AL, Francisco V, Fiacro J, Marcos V, Guillermo C, José DC-R, Guillermo F, Bernardo B (2006) Neuromodulation of the Centromedian Thalamic Nuclei in the Treatment of Generalized Seizures and the Improvement of the Quality of Life in Patients with Lennox-Gastaut Syndrome. Epilepsia 47:1203-1212.

Velasco F, Velasco M, Jimenez F, Velasco AL, Marquez I (2001) Stimulation of the Central Median Thalamic Nucleus for Epilepsy. Stereotact and Funct Neurosurg 77:228-232.

Vergnes M, Marescaux C, Micheletti G, Reis J, Depaulis A, Rumbach L, Warter JM (1982) Spontaneous paroxysmal electroclinical patterns in rat: a model of generalized non-convulsive epilepsy. Neurosci Lett 33:97-101.

Vertes RP (1991) A PHA-L analysis of ascending projections of the dorsal raphe nucleus in the rat. J Comp Neurol 313:643-668.

Vertes RP (1992) PHA-L analysis of projections from the supramammillary nucleus in the rat. J Comp Neurol 326:595-622.

Vertes RP, Martin GF (1988) Autoradiographic analysis of ascending projections from the pontine and mesencephalic reticular formation and the median raphe nucleus in the rat. J Comp Neurol 275:511-541.

Villanueva, Christophe D, Daniel le B, Jean-François B (1998) Organization of diencephalic projections from the medullary subnucleus reticularis dorsalis and the adjacent cuneate nucleus: A retrograde and anterograde tracer study in the rat. J Comp Neurol 390:133-160.

von Krosigk M, Bal T, McCormick DA (1993) Cellular mechanisms of a synchronized oscillation in the thalamus. Science 261:361-364.

Yamasaki DS, Krauthamer GM, Rhoades RW (1986) Superior collicular projection to intralaminar thalamus in rat. Brain Res 378:223-233.

6. Zusammenfassung

Absence Epilepsie ist eine nicht konvulsive Form der Epilepsie, die vorwiegend während der Kindheit auftritt und durch einen Bewusstseinsverlust gekennzeichnet ist. Während eines Anfalls treten im Elektroenzephalogramm (EEG) bilateral synchrone Spike-Wave-Entladungen (SWDs) mit einer Frequenz von 3 Hz auf. Wie frühere Studien zeigen, ist das thalamokortikale Netzwerk, welches die für den Schlaf typischen Oszillationen generiert, auch an der Entstehung der Absence Anfälle beteiligt. Die während der Schlafrhythmen synchronisierte Aktivität des thalamokortikalen Netzwerks erreicht während eines epileptischen Anfalls einen hypersynchronen Zustand, der zu Spitze-Welle-Entladungen führt. Dabei wird der Übergang vom synchronen zum hypersynchronen Zustand im sensorischen Kortex initiiert.

Der Großteil aller Studien die sich mit der Entstehung der SWDs auseinandersetzen konzentriert sich auf den nucleus reticularis (NRT) oder die spezifischen thalamischen Kerne (z.B. corpus geniculatum laterale), obwohl es experimentelle Hinweise darauf gibt, das die unspezifischen intralaminaren thalamischen Nuclei (ILTN) als Schrittmacher der Spitze-Welle-Entladungen fungieren. Ziel der vorliegenden Studie war es daher, die ILTN mit Hinblick auf ihre mögliche Funktion als Schrittmacher der SWDs zu untersuchen.

Die Experimente wurden *in vivo* an Wistar albino Glaxo Ratten von Rijswijk (WAG/Rij), einem gut etablierten Tiermodell für Absence Epilepsie, durchgeführt. Die Tiere befanden sich während der Versuche in einer Neurolept-Anästhesie. Die Experimente umfassten extrazelluläre Ableitungen, microiontophoretische Applikationen und Mikrostimulationen im centrolateralen und paracentralen nucleus (CL und PC) des intralaminaren Thalamus.

Unsere Ergebnisse der extrazellulären Ableitungen zeigen zwei unterschiedliche Feuermuster im CL und PC. Während die Neurone im CL burst-ähnliche Aktivität aufweisen, die mit der Wellen-Komponente der Spitze-Welle-Entladungen korreliert, zeigen die Neurone im PC tonische Aktivität, die während der Spitzenkomponente der SWDs gehemmt wird. Wie in dieser Arbeit mit Hilfe microiontophoretischer Applikationen für Neurone im PC nachgewiesen werden konnte, sind sowohl $GABA_A$ als auch $GABA_B$ Rezeptoren an der neuronalen Aktivität während der Spitze-Welle-Entladungen beteiligt.

Die unterschiedlichen Feuermuster von Neuronen des CL und PC lassen vermuten, dass beiden Arealen eine unterschiedliche Funktion zukommt. Bestätigt wird diese Annahme durch die in dieser Studie durchgeführten Mikrostimulationsexperimente. Während Stimulationen im PC Spitze-Welle-Entladungen in Abhängigkeit von der Frequenz entweder hervorrufen oder unterdrücken konnten, hatten Stimulationen im CL keinen Einfluss auf die Spitze-Welle-Entladungen.

Insgesamt sind die gewonnenen Ergebnisse wenig mit der Hypothese zu vereinbaren, dass ILTN als Schrittmacher für SWDs dienen könnten. Die Ergebnisse deuten hingegen darauf hin, dass neuronale Aktivität in ILTN unterdrückt werden muss, damit Spitze-Welle-Entladungen auftreten können.

7. Abbreviations

ACSF	artificial cerebrospinal fluid
AMPA	α-amino-3-hydroxyl-5-methyl-4-isoxazole-propionate
APV	D-2-amino-5-phosphonopentanoate
AVVL	anteroventral ventrolateral thalamic nucleus
B	Bregma
CL	centrolateral thalamic nucleus
CM	centromedian thalamic nucleus
DNQX	6,7-dinitroquinoxaline-2,3-dione
ECoG	electrocorticogram
EEG	electroencephalogram
EPSP	exhibitory postsynaptic potential
GABA	Gamma-aminobutyric acid
GAERS	genetic absence epilepsy rats from Strasbourg
HVA	high voltage activated
I	Intraaural
I_{CAN}	Ca^{2+}-activated nonselective cation current
I_h	hyperpolarization activated cAMP sensitive cation current
ILTN	intralaminar thalamic nuclei
IPSP	inhibitory postsynaptic potential
I_T	T-type Ca^{2+} current
L	Lambda
LTS	low threshold Ca^{2+} spike
LVA	low voltage activated
NMDA	N-methyl-D-aspartic acid
NRT	nucleus reticularis
PBS	phosphate buffered saline

PC	paradcentral thalamic nucleus
Pf	parafascicular thalamic nucleus
PSTH	Peri-Stimulus-Time-Histogram
SC	superior colliculus
SEM	standard error of mean
SWD	spike and wave discharge
VB	ventrobasal thalamus
VL	ventrolateral thalamic nucleus
VPL	venteroposterolateral thalamic nucleus
VPM	venteroposteromedial thalamic nucleus
WAG/Rij	Wistar albino Glaxo rat of Rijswijk

8. Danksagung

Eine Doktorarbeit entsteht selbstverständlich nicht ohne die Unterstützung vieler helfender Menschen. So danke ich im Einzelnen:

Prof. Dr. Hans-Christian Pape für die Möglichkeit, mich innerhalb einer hervorragenden Infrastruktur mit dem Thema der Absence Epilepsie im Rahmen einer Doktorarbeit auseinanderzusetzen.

Prof. Dr. Norbert Sachser für die Bereitschaft, mich bei dieser Arbeit als Gutachter des Fachbereichs Biologie zu betreuen.

Prof. Dr. Ali Gorji für die Einarbeitung in intrazelluläre Ableitungen in vivo. Auch die theoretische Einführung in das Thema wurde mir durch seine geduldigen Erklärungen sehr erleichtert.

Dr. Thomas Seidenbecher, der mich in die Kunst der extrazellulären Ableitungen und der Mikroiontophorese einführte und bereitwillig Komponenten seines Setups zur Verfügung stellte. Seine Hilfestellungen und Ratschläge halfen mir, in kritischen Momenten nicht den Überblick zu verlieren.

Elisabeth Boening, die wohl beste Assistentin die man sich wünschen kann. Ohne ihre Hilfe wäre die Durchführung der Experimente so nicht möglich gewesen. Ihre Unterstützung in allen Bereichen des Lebens war und ist phänomenal.

Dr. Philippe Coulon für die kritische Durchsicht der vorliegenden Arbeit. Mein Englisch wäre ohne seines nicht denkbar.

Prof. Dr. Thomas Budde, Dr. Philippe Coulon und Dr. Tatjana Kanyshkova für das wirklich sehr angenehme Büroklima und den feinen schwarzen Humor.

9. Tabellarischer Lebenslauf